Self-supervised learning for point cloud data: A survey

Changyu Zeng [a,b,c], Wei Wang [b], Anh Nguyen [c], Jimin Xiao [d], Yutao Yue [a,b,c,*]

[a] *Institute of Deep Perception Technology, JITRI, Wuxi, 214000, China*
[b] *Department of Computing, School of Advanced Technology, Xi'an Jiaotong-Liverpool University, Suzhou, 215123, China*
[c] *Department of Computer Science, University of Liverpool, Liverpool, L69 7ZX, United Kingdom*
[d] *Department of Intelligent Science, School of Advanced Technology, Xi'an Jiaotong-Liverpool University, Suzhou, 215123, China*

ARTICLE INFO

ABSTRACT

3D point clouds are a crucial type of data collected by LiDAR sensors and widely used in transportation applications due to its concise descriptions and accurate localization. Deep neural networks (DNNs) have achieved remarkable success in processing large amount of disordered and sparse 3D point clouds, especially in various computer vision tasks, such as pedestrian detection and vehicle recognition. Among all the learning paradigms, Self-Supervised Learning (SSL), an unsupervised training paradigm that mines effective information from the data itself, is considered as an essential solution to solve the time-consuming and labor-intensive data labeling problems via smart pre-training task design. This paper provides a comprehensive survey of recent advances on SSL for point clouds. We first present an innovative taxonomy, categorizing the existing SSL methods into four broad categories based on the pretexts' characteristics. Under each category, we then further categorize the methods into more fine-grained groups and summarize the strength and limitations of the representative methods. We also compare the performance of the notable SSL methods in literature on multiple downstream tasks on benchmark datasets both quantitatively and qualitatively. Finally, we propose a number of future research directions based on the identified limitations of existing SSL research on point clouds.

1. Introduction

With the rapid development of 3D data processing technologies, an increasing number of relevant applications have emerged in both industrial and daily usage, such as Simultaneous Localization and Mapping (SLAM) (Kazerouni, Fitzgerald, Dooly, & Toal, 2022), autonomous driving (Li et al., 2020), and data-driven robotic visual grasping detection (Tian et al., 2022). LiDAR is one of the indispensable types of sensors to capture disordered 3D point cloud data from traffic scenes, which has enabled more challenging tasks like pedestrian detection (Matti, Ekenel, & Thiran, 2017) and road (Wu, Zhou, Zhao, Yue, & Keutzer, 2019) or remote sensing (Yuan, Shi, & Gu, 2021) semantic segmentation based on the strong inference ability of deep neural networks (DNNs).

However, several well known problems in the supervised point cloud DNNs hinder their further development and practical uses. For example, accurate environment perception via DNNs requires millions of labeled data as the input, while point cloud annotating is labor-intensive and time-consuming due to its disordered and sparse nature (Dai et al., 2017). Besides, manual labeling by human experts

or users inevitably leads to mistakes such as mislabeling and omission. Another long-standing problem is that the supervised learning paradigm struggles to capture the underlying patterns of new data and fails to generalize the pre-training model to downstream tasks because of overfitting caused by noisy labels (Sariyildiz, Kalantidis, Alahari, & Larlus, 2022).

The aforementioned issues motivate research in extracting effective feature representations from point clouds via Self-Supervised Learning (SSL) to learn implicit while better representations without manual annotations. Not only does it solve the problem of the error-prone and expensive labeling process, but also relieve the domain adaptation (DA) issues (Csurka, 2017) with improved model generalization ability. Under the SSL paradigm, basic geometric as well as advanced semantic information can be extracted as knowledge and migrated to downstream tasks under the transfer learning setup. This process approximates human learning that discovers objective principles of the world by observing phenomena and summarizing them into a system of experience and knowledge.

* Corresponding author at: Institute of Deep Perception Technology, JITRI, Wuxi, 214000, China.
E-mail addresses: changyu.zeng17@student.xjtlu.edu.cn (C. Zeng), wei.wang03@xjtlu.edu.cn (W. Wang), anh.nguyen@liverpool.ac.uk (A. Nguyen), Jimin.Xiao@xjtlu.edu.cn (J. Xiao), yueyutao@idpt.org (Y. Yue).
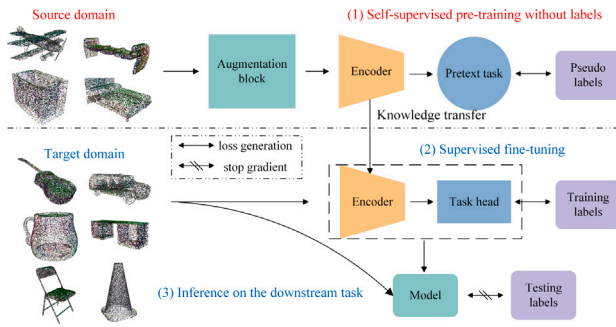
Fig. 1. The general pipeline of SSL used in the point cloud data. (1) Pre-training stage: point cloud data is firstly pre-processed through the augmentation block and then fed into the point-specific encoder to learn feature representations. The features are utilized to complete well-design pretext tasks, where the output will be compared with the pseudo labels derived from the original data to generate a loss and to update encoder parameters via back-propagation; (2) Supervised fine-tuning stage: the well-trained encoder is transferred to the target domain. A task head is trained with the training labels in a supervised manner to complete the downstream tasks; (3) Inference stage: the encoder and task head are concatenated as a model to execute inference on the test set. The effectiveness of the SSL pre-training framework can be evaluated based on the performance of the model on the downstream tasks.

Fig. 2. Taxonomy of SSL for point cloud data based on pretext tasks.

Fig. 1 shows a general pipeline of SSL on point cloud data. The goal of SSL is to pre-train an encoder on an unlabeled, large-scale point cloud dataset (source domain), and to transfer the well-trained network to other datasets (target domain) in various downstream tasks. A complete SSL framework usually contains the following important modules.

- **Data augmentation**: The raw input is augmented via some easy-to-implement pre-processing operations such as translation, rotation, flip, and adding noise (Zhang, Lin, Li, Jia and Zhang, 2022). The objective is to expand the size and diversity of the raw data and to provide subjects for subsequent pretext tasks. The details will be discussed in Section 2.5.
- **Encoder**: The encoder is a point-specific deep network that captures the hierarchical representation of the input point cloud data. We will introduce some commonly used point cloud encoders that learn either from downsampling layer-by-layer (Qi, Su, Mo and Guibas, 2017; Qi, Yi, Su and Guibas, 2017) or local areas to capture the association between different blocks (Wang et al., 2019; Zhou & Tuzel, 2018). The details will be discussed in Section 2.6.
- **Pretext task**: At the core of the framework is the design of a pretext task that mines the hidden self-supervision signal via the interactions between the encoder and data. This part is also the focus of the survey and will be discussed in detail in Section 3.
- **Knowledge transfer**: The well-trained encoder will be transferred to another dataset with the knowledge gained in the source domain after completing the pretext task. A task head is constructed and trained by a small amount of labeled data in the target domain as the supervision signals to fine-tune the whole architecture. The details will be discussed in Section 4.
- **Downstream task**: To evaluate the effectiveness of the SSL framework, the pre-trained encoder will be transferred and evaluated on another dataset for performance evaluation, e.g. object classification, part segmentation, and object detection. The details will be discussed in Section 4.

Thriving progress has been made on point cloud SSL recently, and new models, algorithms and benchmark datasets are emerging quickly and continuously. A systematic review on this exciting topic, especially the research published in the past three years, is urgently needed. In our study, we find that the survey in Xiao, Huang, Guan, and Lu (2022) employed a similar methodology but focused on unsupervised
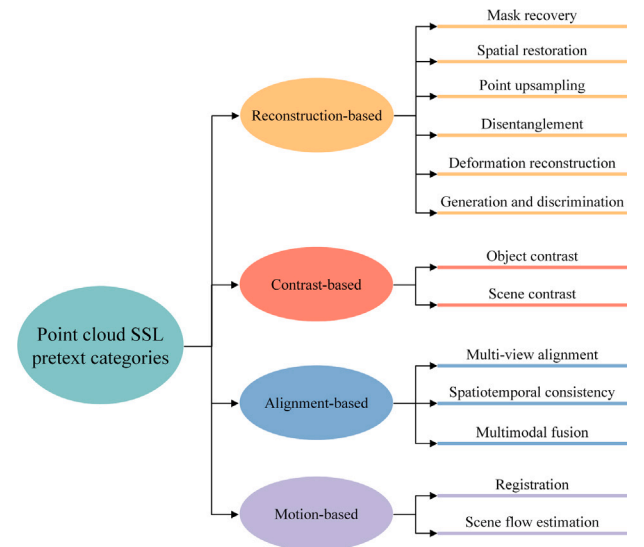
representation learning. However, it lacked a review on the state-of-the-art SSL models, and in particular, a detailed demonstration of most recent published works. Therefore, we are motivated to provide a comprehensive review on the recently published, representative research on point cloud SSL. Our contributions can be summarized as follows:

- **Systematic and novel taxonomy:** We propose a novel and systematic taxonomy for categorizing the diverse kinds of point cloud SSL methods to provide a clear and holistic view on the state of the art. Taking into consideration the characteristics of popular pretext tasks, the taxonomy groups current methods into four broad categories. Each broad category is further subdivided into more fine-grained sub-categories according to the methods in feature utilization as shown in Fig. 2.
- **Comprehensive and detailed summary:** We conduct a comprehensive review of the state of the art, including the background of SSL and point clouds, commonly used datasets and models, pretext tasks, and downstream tasks with performance comparison.
- **Exhaustive dataset summary and evaluation comparison:** We summarize the unique characteristics of 18 most frequently utilized datasets in the point cloud research. More importantly, we compare the performance of different SSL methods on these datasets according to various downstream tasks.
- **Future directions:** Based on our investigation, we summarize and discuss the major limitations and challenges in the current research and propose potential future directions which would hopefully motivate more theoretical and practical research towards more intelligent and effective SSL approaches for point cloud data processing.

The rest of the paper is organized as follows: Section 2 introduces the preliminaries for this survey to equip the readers with the necessary background knowledge on SSL and point cloud data. Section 3 represents the main body of the study and provides an exhaustive and detailed analysis on the state of the arts methods according to the structure of the proposed taxonomy. Section 4 illustrates an evaluation and comparison study on the performance of different SSL methods on the frequently utilized downstream tasks and benchmark datasets. Section 5 discusses the limitations and challenges of current research and proposes potential future directions, and Section 6 concludes the paper.

2. Background

This section will introduce the preliminaries relevant to this survey, including the background of SSL, SSL evaluation criteria, properties of point cloud data, commonly used SSL datasets and models. Additionally, diverse techniques employed in the SSL pipeline, such as point cloud data augmentation, pseudo-label generation and loss function optimization, will be discussed in detail to provide a comprehensive understanding of the SSL framework.

2.1. Self-supervised learning for languages and images

We firstly describe the development history of SSL in the language and image domains. The purpose is to provide readers a general understanding on SSL. Although data types vary from domains to domains, the core idea of SSL remains the same: to leverage data characteristics for transformation processing and to make the transformed data consistent with the original input in terms of feature representation by contrasting or reconstruction.

The idea of SSL was firstly introduced in Natural Language Processing (NLP) research. After converting words into vectors, e.g. Word2Vec (Mikolov, Chen, Corrado, & Dean, 2013), and utilizing the relationships between the representations and context, models could learn semantic representations from neighboring words or sentences through pretext task formulations such as next sentence prediction (Devlin, Chang, Lee, & Toutanova, 2018), auto-regressive language modeling (Floridi & Chiriatti, 2020), or sentence permutation (Lewis et al., 2019). Landmark models such as GPT (Floridi & Chiriatti, 2020) and BERT (Devlin et al., 2018), and many variants celebrate great achievements in not only NLP but also other fields later.

In the field of image processing and computer vision, different SSL methods impose simple variations on image data and extract features by recovering it to the original input, for example, from simple tasks like relative position prediction (Doersch, Gupta, & Efros, 2015; Noroozi & Favaro, 2016) and rotation angle prediction (Gidaris, Singh, & Komodakis, 2018), to reconstructing blocks masked by surrounding visible pictures (He et al., 2021; Pathak, Krähenbühl, Donahue, Darrell, & Efros, 2016). Free semantic label-based (Croitoru, Bogolin, & Leordeanu, 2017; Faktor & Irani, 2014; Jiang, Larsson, Shakhnarovich, & Learned-Miller, 2018; Stretcu & Leordeanu, 2015) and cross-modal-based methods (Agrawal, Carreira, & Malik, 2015; Arandjelovic & Zisserman, 2017; Jayaraman & Grauman, 2015) have been proposed, which learn representations via automatically generated semantic labels and extra information from other modalities. Recently, the research community shows a great interest on contrastive learning (Caron et al., 2020; Chen, Kornblith, Norouzi, & Hinton, 2020; He, Fan, Wu, Xie, & Girshick, 2020), which aims to differentiate positive and negative samples by comparison using data augmentation techniques. These research works inspired the study of SSL on point clouds, with similar ideas transferred from 2D to 3D by adapting for data peculiarities.

2.2. Self-supervised learning evaluation criteria

Harmonized and standardized evaluation criteria are vital for pre-trained models under different proxy pretexts in SSL. This section will introduce the commonly used evaluation metrics for SSL in computer vision, including both image and point cloud data.

Similar to the supervised paradigm, a generic evaluation criterion for assessing the quality of an SSL model is its performance on specific tasks. A typical method to evaluate SSL models is to freeze the pre-trained encoder and report the result of a linear probing trained to solve classification problems, for example, using ImageNet (Russakovsky et al., 2015) or ModelNet (Wu et al., 2015) for image and point cloud data, respectively. To comprehensively assess the transfer performance on a broader range of tasks rather than predictive tasks, Ericsson, Gouk, and Hospedales (2021) proposed to evaluate pre-trained models on different downstream tasks under different settings, such as full and few-shot classification measured by Overall Accuracy (OA) or Mean Class Accuracy (mAcc), part and semantic segmentation measured by mean Intersection over Union (mIoU), and object detection measured by Average Precision (AP). Moreover, the evaluation protocol may not be restricted to the linear probing formality only, but contain fine-tuning (re-training), where the pre-trained model serves as the initial downstream encoder for feature extraction. The performance of the pre-trained model on downstream tasks is the mainstream evaluation criterion for SSL methods in the computer vision domain and will be reported in detail in Section 4.

2.3. Properties of point cloud data

Data properties are distinct between naturals languages, images, and point clouds. Languages are usually complex and abstract in nature, and contain ambiguous information due to its versatility and richness. It is expressed in a sequence of words, which is discrete and unstructured in the representation space (He et al., 2020). In contrast, images contain rich visual information, such as color, texture, and shape information of an object in high-dimensional space (Jing & Tian, 2020) for human perception. They are usually represented as 2D data by using a matrix of pixel values.

Simply speaking, point cloud data is similar to image data in terms of visual format and can be regarded as 3D stereo images with depth information. However, the attributes of point cloud data are completely different in geometric representation. Specifically, a point cloud is a collection of discrete, disordered, and topology-free 3D points. The most basic information contained in the points is the position coordinates (x_i, y_i, z_i) in the Euclidean space, where i is the number of points in the object. There are also other optional attributes such as color, intensity, reflectivity, etc., specifying physical properties of the points in more detail. The input order is trivial for point cloud data and does not impact the semantic meaning while it is crucial for images and language where various words or pixel sequences lead to completely divergent connotations. Additionally, point cloud data is invariant to rigid transformation, which means that it remains unchanged after rotation and translation. Some of such exclusive properties can be summarized as follows:

- **Sparsity:** The point cloud data is discretely distributed on the surface of the scanned object or scene.
- **Non-uniformity:** The distance between points is not fixed and is determined by various factors such as the instruments' sampling strategy, relative position, and scanning range.
- **Incomplete data:** Some parts of real-scanned surfaces are incomplete due to self or external occlusion.
- **Noise:** It is inevitable that noise from environmental factors or inaccuracies in instruments will be present.
- **Permutation invariance:** The order of points does not affect the overall semantic representation of point cloud objects, so identical point cloud objects can be expressed by various matrices.
- **Transformation immutability:** Point clouds remain immutable through rigid transformations such as rotation and translation.
- **Points interaction:** There are correlations, either strong or weak, between points in global and local regions.

2.4. Point cloud dataset

Quality benchmark datasets (e.g. complete, well-varied, and densely-labeled) play essential roles in SSL research. This section lists the most commonly used point cloud datasets and summarize them in Table 1 in terms of sample number, object categories, suitable tasks, and highlights. These datasets may contain synthetic and real scanned data, in single frames and time series and from individual objects

Table 1

Summary of commonly used point cloud datasets. Abbreviations for suitable tasks: Cls (Classification); Seg (Semantic Segmentation); Det (Object Detection); Com (Semantic Scene Completion); Rec (Surface Reconstruction); CM (Cross-Modal tasks); Pos (Pose estimation); Tra (Object Tracking).

Year	Name	#Samples	#Categories	Types	Suitable tasks	Highlights
2012	KITTI (Geiger, Lenz, & Urtasun, 2012)	Over 200k objects	8	RGB	Cls/Det/CM	Comprehensive outdoor driving dataset
2015	ModelNet (Wu et al., 2015)	12,311 models	40	CAD	Cls/Seg/Rec	Frequently used in classification and few-shot
2015	ShapeNet (Chang et al., 2015)	57,448 models	55	CAD	Cls/Seg	Commonly employed as the pre-training dataset
2015	SUN RGBD (Song, Lichtenberg, & Xiao, 2015)	10,335 images	37	RGB-D	Seg/Det/Pos	A RGB-D scene understanding benchmark suite
2016	SceneNN (Hua et al., 2016)	100 scenes	–	RGB-D	Det/Rec/Pos	Using unique triangle meshes shape contour
2016	ObjectNet3D (Xiang et al., 2016)	44,147 shapes	100	CAD	Det/CM/Pos	Well-aligned 2D-3D dataset
2016	S3DIS (Armeni et al., 2016)	272 scans	13	Point	Cls/Seg/CM	Large-scale indoor space scanning dataset
2017	ScanNet (Dai et al., 2017)	1513 scenes	20	RGB-D	Cls/Seg/Com	Rich labels for scene understanding tasks
2017	Semantic3D.net (Hackel et al., 2017)	Over 4B points	8	Point	Cls/Seg/Det	High quality resolution and scope outdoor dataset
2018	Pix3d (Sun et al., 2018)	10,069 3D-2D pairs	9	CAD	Rec/CM/Pos	Pixel-level image-shape pairs dataset
2019	ABC (Koch et al., 2019)	1M objects	–	CAD	Seg/Rec	Providing a benchmark for surface normal estimation
2019	ScanObjectNN (Uy, Pham, Hua, Nguyen, & Yeung, 2019)	2902 objects	15	Point	Cls/Seg	Challenging real-world scenario with noise
2019	PartNet (Mo et al., 2019)	26,671 models	24	Points	Seg/Rec	Producing fine-grained multi-level 3D part objects
2020	RobustPointSet (Taghanaki et al., 2020)	73,843	40	Mesh	Cls	Benchmark to evaluate the robustness of classifiers
2020	Waymo (Sun et al., 2020)	12M objects	–	Point	Det/CM/Tra	Suitable for cross-modal and transfer learning
2020	NuScenes (Caesar et al., 2020)	1k scenes	23	Point	Det/CM/Tra	Containing additional annotations and scenes
2021	SensatUrban (Hu et al., 2021)	4B points	13	Point	Seg	Data collected by UAV over UK landscape
2022	STPLS3D (Chen et al., 2022)	62 scenes	18	Point	Seg/Det	Covering both real and synthetic aerial point clouds

and complex scenes. There are also a few datasets for complex traffic scenarios (e.g. automatic driving) containing extra data in different modalities, such as from images or radars.

- **KITTI** (Geiger et al., 2012) is a benchmark suite for autonomous driving vision tasks. The dataset was collected using several pieces of equipment, including four video cameras, a laser scanner, and a localization system. It includes not only point clouds but also stereo and optical flow data. There are more than 200,000 annotated point cloud scenarios consisting of cars and pedestrians, providing a novel and challenging benchmark for 3D object detection and orientation estimation.

- **ModelNet** (Wu et al., 2015) is the most widely used 3D point cloud CAD dataset for object classification and few-shot learning. It contains 12,311 single objects from 40 categories, with each point composed of six dimensions of information, including XYZ spatial coordinates and RGB values.

- **ShapeNet** (Chang et al., 2015) is a relatively large-scale repository of 3D CAD objects frequently employed as a pre-training dataset. It contains more than 3 million samples categorized into 55 classes under the WordNet synsets (Miller, 1995) criteria. The annotations in the dataset are versatile, including rigid alignments, parts, physical sizes, and key points.

- **SUN RGBD** (Song et al., 2015) is an RGB-D scene understanding benchmark suite containing 10,335 samples at a comparable scale to PASCAL VOC (Everingham, Van Gool, Williams, Winn, & Zisserman, 0000). It has 146,617 2D polygons and 64,595 3D bounding boxes densely annotated to indicate object orientation, room layout, as well as scene category for overall scene awareness.

- **S3DIS** (Armeni et al., 2016) is a 3D indoor venue dataset that consists of scanning of 272 rooms in 6 areas overlaying a 6000 m² area. It has 13 semantic categories labeled by fine-grained point-wise annotations carrying full 9D information, including XYZ, RGBs, and normalized location coordinates.

- **ScanNet** (Dai et al., 2017) is a 3D RGB-D dataset that comprises 2.5M views in 1513 scenes acquired in 707 indoor environments. Various tests containing semantic voxel labeling and CAD model retrieval proved that ScanNet provides quality data for 3D scene understanding.

- **ScanObjectNN** (Uy et al., 2019) was proposed as a collection of real-world indoor point cloud scenes to break the performance saturation of 3D object classification on synthetic data.
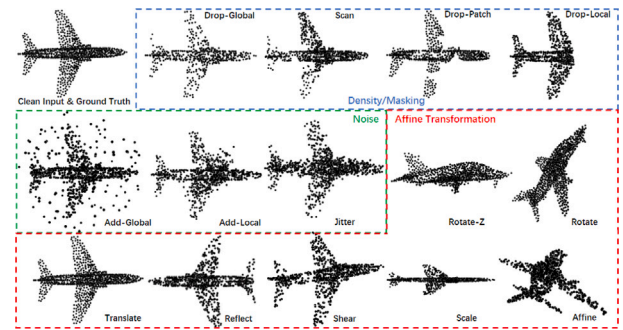

Fig. 3. Illustration of the commonly used data augmentation methods for point cloud data. There are a total of 14 sub-categories of data augmentation methods that could be classified as three general corruption families.
Source: The figure is adapted from Zhang, Lin, Li et al. (2022).

This dataset introduces new challenges for 3D object classification due to the presence of background noise and occlusions that require networks' ability on context-based reconstructions and partial observations.

- **Waymo** (Sun et al., 2020) is a large autonomous driving dataset produced by Waymo in collaboration with Google Inc. The dataset consists of 1150 urban and suburban geography scenes spanning 20 s, which are collected via well-synchronized and calibrated LiDARs and cameras.

- **NuScenes** (Caesar et al., 2020) is another remarkable multimodal dataset provided by the full sensor suite including cameras, radars, and LiDARs. Compared to other autonomous driving datasets, it contains additional annotations like pedestrian pose, vehicle state, and also scenes from nighttime and rainy weather.

2.5. Point cloud data augmentation

Data augmentation is a crucial technique for enhancing DNNs performance by increasing the amount and diversity of training samples. For SSL tasks, it not only prevents the model from overfitting but also facilitates capturing robust and invariant representations of point clouds under multiple transformations. In this section, we will introduce the commonly used data augmentation methods and compare the effectiveness of each methods via a metric called task relatedness.
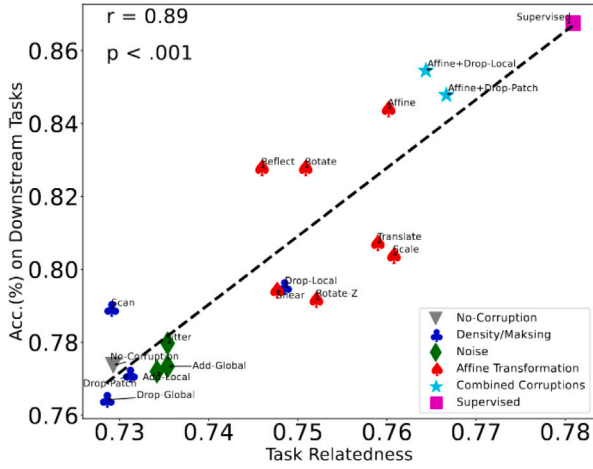
Fig. 4. Illustration of the relationship between task relatedness and classification accuracy on downstream tasks. *r* and *p* are the coefficients to measure the linear relationship and statistical significance for the Pearson correlation, respectively. *Source:* The figure is adapted from Zhang, Lin, Li et al. (2022).

Essentially, data augmentation is a process of generating new data by adding interventions or corruptions without destroying the original semantic expressions. For point clouds, augmentation methods are based on the properties mentioned in Section 2.3 and can be classified into three general groups: density/masking, noise, and affine transformation (Zhang, Lin, Li et al., 2022). These three corruption families could be further divided into 14 sub-categories as shown in Fig. 3.

Density/masking is the most frequent data augmentation method adopted in mask autoencoder (MAE) type SSL research (He et al., 2021; Pang et al., 2022; Yu et al., 2021). Based on the principle that point cloud data is sparse with uneven density, randomly removing a certain percentage of points while preserving part of the semantic expression presents a challenging learning objective for such MAE-based tasks. On the contrary, the noise based methods impose interventions on the original clean input to increase the difficulty of feature extraction. Affine transformation leverages point cloud invariance characteristics to shift the spatial coordinates of each points. This has significant impact on the input since the basic position information completely changes.

The work in Chen et al. (2020) and Zhang, Lin, Li et al. (2022) investigated the effectiveness of the aforementioned augmentation methods as pretext data preprocessing on downstream classification tasks. Task relatedness is employed as the evaluation metric to statistically measure the performance of SSL models on downstream tasks, which provides valuable advice for proxy data augmentation selection. Following (Zamir et al., 2018), for each pretext task *c*, its task relatedness to downstream task *t* is defined as:

$$A_{c \to t} := \mathbb{E}_{x \in X} \mathcal{I}_t(R_c(E_c(x)), f_t(x)) \tag{1}$$

where x is a sample in a point cloud dataset X; E_c is the model's encoder pre-trained on task c; R_c is a readout function, which indicates the classification head composed of several fully connected (FC) layers; f_t is the labeling function; $\mathcal{I}_t$ is accuracy measurement estimating whether the downstream output $R_c(E_c(x))$ conforms to the ground truth $f_t(x)$.

To further explore the relationship between task relatedness and classification accuracy on downstream tasks, Pearson correlation coefficient r and p-value are utilized to estimate the linear relationship as well as statistical significance (Fraser, 1976), respectively, where $|r| > 0.5$ refers to a strong correlation and $p < 0.05$ is considered statistically significant. Fig. 4 demonstrates the statistically significant linear relationship between task relatedness and classification accuracy on downstream tasks when $r = 0.89$ and $p < 0.001$. The results reveal a counterintuitive fact that frequently used density/mask and noise-based data

augmentation methods are ineffective for downstream tasks either in accuracy and task relatedness. Conversely, the seemingly simple affine transformation enhances task relatedness to point cloud classification, resulting in higher accuracy. Furthermore, combining corruptions of affine transformation and mask can approach the performance of supervised benchmarks. Hence, using affine transformation-based methods for data augmentation is preferable for in SSL pre-training.

2.6. Popular deep models for point clouds

SSL techniques designed for languages and images need to be revised and extended for point clouds. For instance, traditional CNN networks cannot handle irregular and discrete point cloud data well since there is no guarantee that a corresponding point exists at the same relative position of the convolution. In this section, we briefly introduce five point cloud networks that are frequently used as feature extraction encoders in the literature. Their architectures are illustrated in Fig. 5.

2.6.1. Point-based models

Point-based models capture point representations at point-wise level. To reduce data size and computation complexity, Qi et al. proposed PointNet (Qi, Su et al., 2017), which is the pioneering work to extract features directly on raw point clouds. It is widely deployed as the feature extractor (Poursaeed, Jiang, Qiao, Xu, & Kim, 2020; Sauder & Sievers, 2019b; Wang, Liu, Yue, Lasenby and Kusner, 2021) due to its simple and lightweight network structure. Taking advantage of the point permutation invariance, PointNet aligns the input points to a canonical space and aggregates global features by symmetric functions such as max pooling.

However, it fails to capture local structures induced by the metric space in which the points reside, thereby limiting its ability to recognize fine-grained patterns and generalize to complex scenes. The updated version PointNet++ (Qi, Yi et al., 2017) was then put forward several months later. It adopts multi-scale, multi-resolution sampling, and groping strategies to propagate features from one level to another, which improves the feature learning ability further. Furthermore, the point patch generation strategy combining Farthest Point Sampling (FPS) and K-Nearest Neighbor (KNN) provides a template for point cloud cropping preprocessing for subsequent studies (Pang et al., 2022; Yu et al., 2021; Zhang et al., 2022).

2.6.2. Voxel-based models

Voxel represents a regular grid to segment 3D space into finite unit cubes. VoxelNet (Zhou & Tuzel, 2018) is a generic point-specific network that uses voxels to divide and access a local representation of point clouds for 3D detection tasks (Hess et al., 2022; Li et al., 2022; Min, Zhao, Xiao, Nie, & Dai, 2022). This network partitions disordered point clouds and performs feature learning in quantified and fixed-size 3D structures. One innovation is the stacking Voxel Feature Encoding (VFE) layers which encode interaction between points within a voxel and grasp descriptive appearance information. The output of each VFE layer is the concatenation of point-wise features and locally aggregated features so that local features are better captured. However, the expensive computation of voxel construction and quantization artifacts constrain the model from capturing high-resolution or fine-grained representations.

2.6.3. Graph-based models

A graph is a data structure consisting of nodes and edges that can represent objects and their relationships. Since it can model intricate interactions between objects, graph has been a natural choice for applications like recommendation systems (Cai, Huang, Xia, & Ren, 2023; Wei, Liang, Liu, & Wang, 2022). Analogously, a local point cloud can also be modeled by a graph network as a point with its neighbors can reflect the geometry property of the points. Wang et al. proposed a dynamic graph-based CNN network (DGCNN) (Wang et al., 2019) that
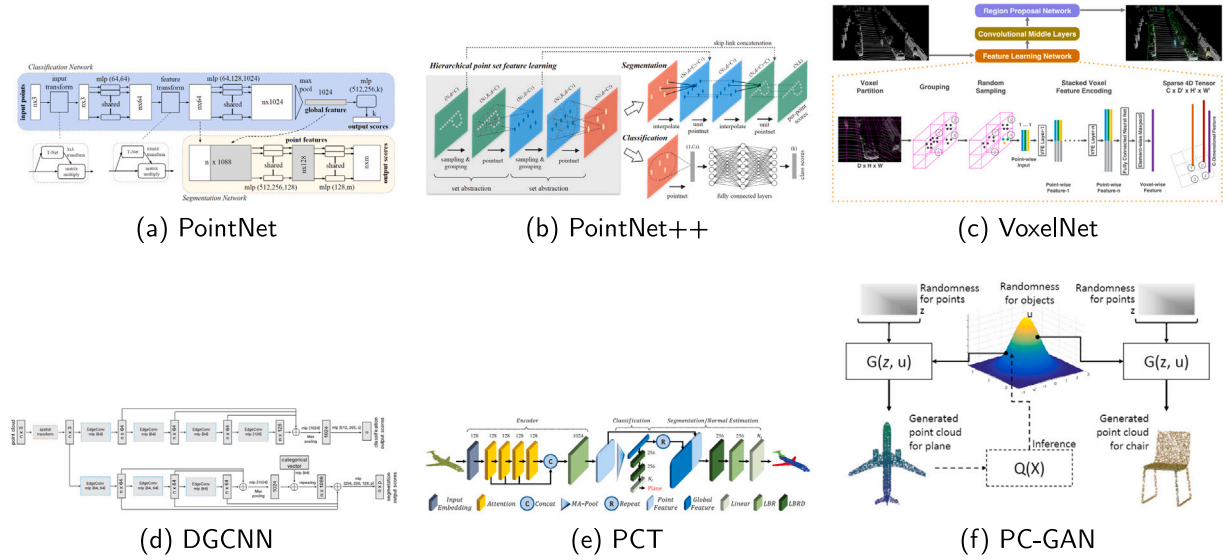
(a) PointNet   (b) PointNet++   (c) VoxelNet

(d) DGCNN   (e) PCT   (f) PC-GAN

Fig. 5. Illustration of the commonly used deep networks for extracting point cloud features.

encodes the edge features between vertices. Instead of learning point representations directly, DGCNN represents the interactions between points and their edges in both Euclidean and semantic space, and learns the graph structure dynamically. This graph network-based architecture has served as a backbone in many subsequent point cloud SSL models with notable results (Afham et al., 2022; Poursaeed et al., 2020; Sauder & Sievers, 2019b).

2.6.4. Transformers-based models

Transformers have become one of the most prevalent architectures in many fields. They benefit from the multi-head self-attention mechanism, which allows them to capture long-range dependencies between point patches and discover implicit regional correlations. The state-of-the-art performance on SSL point cloud classification and part segmentation has been achieved by transformer-based models such as the one proposed by Zhang, Lin, He et al. (2022). Furthermore, point cloud transformer (PCT) (Guo et al., 2021), a variant adapted specifically for point clouds, enhances local feature extraction with the support of farther point sampling and nearest neighbor search, and further improves performance on various downstream tasks.

2.6.5. GAN

Generative Adversarial Network (GAN) (Goodfellow et al., 2014) is a widely used framework in reconstruction-based pretext tasks for point cloud knowledge mining. It consists of two components: the generator, which generates point clouds similar to the training data, and the discriminator, which distinguishes between generated and real points. These two modules are trained under an adversarial paradigm without supervision. The framework can be formulated as a two-player minimax game:

$$\min_{G} \max_{D} E_{x \in X}[log(D(x))] + E_{z \in Z}[log(1 - D(G(z)))] \quad (2)$$

where D and G denotes the discriminator and the generator, and X and Z represent the data and noise distribution, respectively. Furthermore, there are some GANs networks adapted specifically for point clouds, such as PU-GAN (Li, Li, Fu, Cohen-Or, & Heng, 2019), PC-GAN (Li, Zaheer, Zhang, Poczos, & Salakhutdinov, 2018), and RL-GAN (Sarmad, Lee, & Kim, 2019).

2.7. Pseudo labels

Pseudo labels are introduced in point cloud SSL due to the absence of ground truth labels. It facilitates the calculation of loss with the output of the pretext tasks, which is then used for updating encoders via backpropagation. Information contained in pseudo labels is often considered as a more reliable and informative source for pretext tasks to learn point cloud representation than tags. For instance, the label 'airplane' only indicates the shape of objects without descriptions like colors, poses, and differences from other samples in same category. In contrary, these attributes are implicitly contained in point clouds and could be captured as pseudo label in SSL tasks.

Different methods define pseudo labels in different ways. In most reconstruction-based pretext tasks, pseudo labels are point cloud itself which provides a rebuilding objective for pretext task. In contrast-based methods, pseudo labels are a multidimensional matrix carrying collection information and are typically generated using clustering methods such as memory bank (Wu, Xiong, Yu, & Lin, 2018), online dictionary (He et al., 2020), and prototype approaches (Caron et al., 2020), representing mean and variance of all or part of the features of point cloud dataset. For some alignment-based prediction or motion-based tasks pre-trained on temporal point cloud datasets, pseudo labels are geometric information like position, pose, and orientation in a number of frames before and after.

2.8. Loss functions

Appropriate and easily-differentiable loss functions are critical to facilitate backpropagation and optimization for encoders. In reconstruction-based pretext tasks, the symmetric function, Chamfer distance (CD), is commonly employed to assess the distance between each point in one set and its corresponding nearest point in the other. More formally, for two non-empty subsets X and Y, Chamfer distance $d_{CD}(X, Y)$ is defined as:

$$d_{CD}(X, Y) = \frac{1}{|X|} \sum_{x \in X} \min_{y \in Y} \|x - y\|^2 + \frac{1}{|Y|} \sum_{y \in Y} \min_{x \in X} \|x - y\|^2 \quad (3)$$

Here, x and y represent the points in the reconstruction point set X and the original input point set Y, respectively; $\| \cdot \|$ denotes the L2 distance between two points and $| \cdot |$ refers to the number of points. The smaller the CD value, the more similar the two point sets are, and the better the SSL algorithm performs.

For contrast-based pretext tasks, the objective is to discriminate the similarities and differences between each point cloud samples on the overall semantic level. A cross-entropy like loss function to encourage the positive samples to be close to each other (and negative ones to be far from each other) is needed. InfoNCE (NCE stands for Noise-Contrastive Estimation) is a contrastive loss function that estimates the
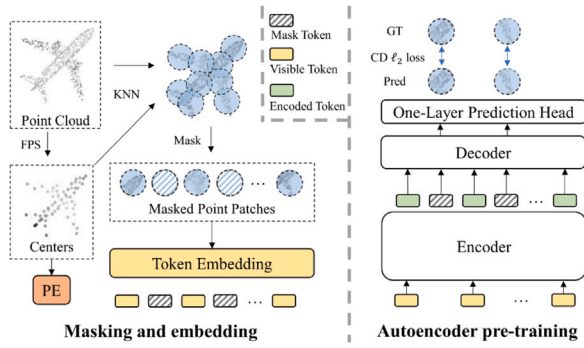
Fig. 6. The general pipeline of Point-MAE. (1) The process of masking and embedding is demonstrated on the left. The point cloud patches are generated by FPS and KNN and masked randomly. Both visible and mask patches are mapped to the corresponding tokens through PointNet-based embedding layers. Also, the Position Embedding (PE) is obtained by mapping the center coordinates to the embedding dimension. (2) The autoencoder pre-training is shown on the right. The encoder only processes the visible tokens while the mask tokens are shifted and added to the input sequence of the decoder to reconstruct the masked patches.
Source: This figure is adapted from Pang et al. (2022).

Fig. 7. Illustration of the CloudContext pretext task. The pre-training model is enforced to estimate the spatial relevance between two given point cloud segments from six categories. In this case, the exact relation of these two components is 'the red part is diagonally above the blue part'.
Source: This figure is adapted from Sauder and Sievers (2019a).

mutual information between a pair of samples, and can be formulated as:

$$L_q = -\log \frac{\exp(q \cdot k_+/\tau)}{\sum_{i=0}^{K} \exp(q \cdot k_i/\tau)} \tag{4}$$

where q indicates the encoded query (feature); k indicates a set of $K + 1$ encoded samples $\{k_0, k_1, k_2, \ldots, k_K\}$, which could be regarded as the prototypes of historical samples; τ is the temperature parameter controlling the sharpness of the distribution. Assuming there is only one positive sample k_+ in the set k matching the query q, the others K samples are all negative. InfoNCE aims to assign the query q into the positive sample k_+ in the $K + 1$ classification problem (He et al., 2020). In other words, the loss function tries to maximize the logits of $q \cdot k_+$ and minimize the value of the denominator.

3. Self-supervised learning pretext tasks for point cloud

We classify the current point cloud SSL research into four general categories based on the nature of the pretext tasks: reconstruction-based, contrast-based, alignment-based, and motion-based methods, as shown in Fig. 2. These categories can be further divided into more fine-grained sub-categories according to the different ways in which the features are extracted and used. The following sections summarize the principles and peculiarities of various proxy tasks in details. It should be noted that some methods may reside in multiple sub-categories.

3.1. Reconstruction-based methods

Reconstruction-based methods learn point cloud representations by reconstructing the corrupted point clouds and recovering the original ones as much as possible. Global features as well as the mappings between local and global areas are learned during the reconstruction process. According to different types of corruption and reconstruction objects, we further divide them into six sub-categories: mask recovery, spatial restoration, point sampling, disentanglement, deformation reconstruction, and generation and discrimination. Summary about the methods under these six sub-categories is shown in Table 2.

3.1.1. Mask recovery
The core idea of reconstruction is to mask a portion(s) of the point cloud and recover such missing part via an encoder–decoder architecture. Similar to the image inpainting task (Sarmad et al., 2019) and Mask AutoEncoder (MAE) (Hess et al., 2022), the encoder is
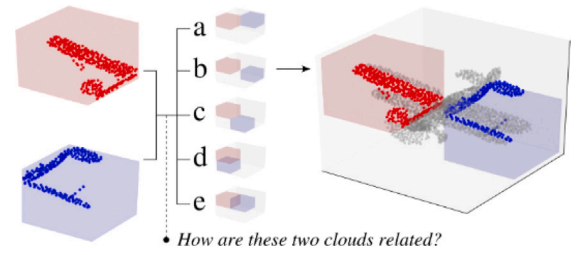
required to capture the local geometric structure and the regional relations during the restoration process. Generally speaking, the better the reconstruction, the more effective the learned features.

Point-BERT (Yu et al., 2021), built based on BERT (Devlin et al., 2018), designs a point-specific tokenizer on discrete Variational AutoEncoder (dVAE) to map patches to discrete tokens to capture meaningful local geometric patterns. A portion of the input is randomly masked out, and a BERT-style transformer is trained to reconstruct the missing token under the supervision of point tokens obtained by the tokenizer. However, the tokenizer should be pre-trained in advance, and Point-BERT over-relies on auxiliary contrastive learning as well as data augmentation.

To address this issue, Pang et al. proposed Point-MAE (Pang et al., 2022) as a neat and efficient scheme of mask autoencoder as shown in Fig. 6. Concretely, Point-MAE employs the standard transformer as the backbone with an asymmetric encoder–decoder architecture to process random masking points with a high ratio (60%–80%). The mask tokens are shifted from the input of the encoder to the lightweight decoder, which saves considerable computation, and more significantly, avoids early leakage of location information. To further capture local geometric information, Zhang et al. introduced Mask Surfel Prediction (MaskSurf) (Zhang, Lin, He et al., 2022), which estimates the surfel position (i.e., points) and per-surfel orientation (i.e., normals) simultaneously. Such a two-head pre-training paradigm has been justified to capture more effective representations than a reconstruction-only pretext. Likewise, Voxel-MAE (Min et al., 2022) transforms point clouds into volumetric representations and applies the range-aware random masking strategy on the voxel grid. Besides reconstructing the occupancy value of masked voxels, a supplementary binary voxel classification task distinguishing whether the voxel contains point clouds boosts the model to learn more complicated semantics.

3.1.2. Spatial restoration
Point clouds are the coordinate sets containing abundant spatial information that describes the structural distribution of objects and the environment in the Euclidean space. It is natural to exploit such rich spatial knowledge as the supervision signal in pretext tasks.

Sauder and Sievers (2019b) proposed a 3D version of the jigsaw pretext to rearrange point clouds whose parts have been randomly disrupted and displayed by voxels along the axes. The goal of this pretext is to restore the original position of each patch (labeled by voxel ID) from the state of chaotic and disorderly distribution. They later developed CloudContext (Sauder & Sievers, 2019a) to forecast the spatial relevance between two point cloud segments. As shown in Fig. 7, the model is trained to predict the relative structural position between two given patches from the same object, which utilizes the innate attributes of point clouds as they are not restrained by a discrete grid. By doing so, powerful per-point features can be accessed in an easy-to-implement unsupervised manner without expensive computation.

Table 2
Summary of reconstruction-based point cloud SSL methods. D & G stand for generation and discrimination.

Year	Method	Sub-categories	Contributions
2021	Point-BERT (Yu et al., 2021)	Mask recovery	Reconstructing missing point tokens with BERT-style transformer
2022	Point-MAE (Pang et al., 2022)	Mask recovery	Shifting masked tokens to decoder to avoid early leakage
2022	MaskSurf (Zhang, Lin, He et al., 2022)	Mask recovery	Estimating surfel position and per-surfel orientation simultaneously
2022	Voxel-MAE (Min et al., 2022)	Mask recovery	Performing additional binary voxel classification for complicated semantics awareness
2019	3D jigsaw (Sauder & Sievers, 2019b)	Spatial restoration	Rearranging randomly disorganized point clouds
2019	CloudContext (Sauder & Sievers, 2019a)	Spatial restoration	Predicting relative structural position between two given patches
2020	Orientation estimation (Poursaeed et al., 2020)	Spatial restoration	Predicting and recovering rotation angle around an axis
2019	PU-GAN (Li et al., 2019)	Point upsampling/D & G	Utilizing self-attention unit for feature aggregation and quality enhancement
2021	SSPU-Net (Zhao, Hui, & Xie, 2021)	Point upsampling	Leveraging shape coherence between sparse input and generated dense point cloud
2022	UAE (Zhang, Shi, Deng and Wu, 2022)	Point upsampling	Gaining both advanced semantic information and basic geometric structure
2022	SPU-Net (Liu, Liu, Liu and Han, 2022)	Point upsampling	Integrating self-attention with graph convolution network for context feature extraction
2022	PUFA-GAN (Liu, Yuan, Hou, Hamzaoui and Gao, 2022)	Point upsampling/D & G	Employing graph filter to extract high frequency points of sharp edges and corners
2022	SSAS (Zhao et al., 2022)	Point upsampling	Achieving magnification-flexible point clouds upsampling
2022	Pose Disentanglement (Tsai, Chiang, Tsai, & Chiu, 2022)	Disentanglement	Uncoupling content and pose attributes in partial point clouds
2022	CP-Net (Xu, Zhou, Xu, Wang, & Qiao, 2022)	Disentanglement	Disentangling point clouds into contour and content ingredients
2022	MD (Sun, Zheng, Wang, Xu, & Yang, 2022)	Disentanglement	Separating mixing point cloud into two independent objects
2018	FoldingNet (Yang, Feng, Shen, & Tian, 2018)	Deformation reconstruction	Stretching 2D grid lattice to reproduce 3D surface structure
2019	Graph topology (Chen et al., 2019)	Deformation reconstruction	Learning pairwise relationships between points and refine coarse reconstructions
2021	Self-correction (Chen et al., 2021)	Deformation reconstruction	Recovering shape-disorganized point regions
2021	DefRec (Achituve, Maron, & Chechik, 2021)	Deformation reconstruction	Performing deformation on 2D grids to fit arbitrary 3D object surface
2018	PC-GAN (Li et al., 2018)	D & G	Employing hierarchical and interpretable sampling strategy
2019	RL-GAN (Sarmad et al., 2019)	D & G	Introducing reinforcement learning agent to control GAN
2019	TreeGCN (Shu, Park, & Kwon, 2019)	D & G	Leveraging ancestor information to boost point representation
2022	MaskPoint (Liu, Cai and Lee, 2022)	D & G	Performing simple binary classification as proxy task
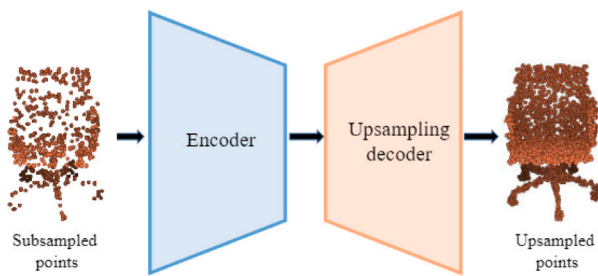
Fig. 8. Overview of Upsampling AutoEncoder. The input point cloud is subsampled by a random sampling strategy and then fed into the encoder to extract point-wise features. The decoder is adopted to reconstruct the original point cloud with offset attention based on the learned representation.
Source: This figure is adapted from Zhang, Shi et al. (2022).

Orientation estimation (Poursaeed et al., 2020) is another simple but effective proxy task to capture the spatial information of point clouds. With the canonical orientation provided in most datasets, the orientation estimation pretext task aims to predict and recover the rotation angle around an axis via matrix multiplication. Such a pretext requires a high-level holistic understanding of shapes and obviates the need for manual annotations.

3.1.3. Point upsampling

Point upsampling is the operation to upsample sparse, noisy, and non-uniform point clouds to generate a dense, complete, and high-resolution point cloud, which is challenging but also beneficial for the model to capture implicit geometric representations of the underlying surface.

PU-GAN (Li et al., 2019) is a pioneer SSL upsampling paradigm formulated based on the generative adversarial network (GAN) (Goodfellow et al., 2014) to generate a diverse range of point distributions from the latent space and upsample points over patches. An up-down-up unit is embedded in the generator to expand point features as well as a self-attention unit for quality enhancement on feature aggregation. The discriminator is inspired to gain inherent patterns and improve the uniformity of output generation according to a compound loss including adversarial, uniform, and reconstruction terms. Motivated by PU-GAN, Zhang et al. proposed the Upsampling AutoEncoder (UAE) (Zhang, Shi et al., 2022) to gain both advanced semantic information and basic geometric structure from subsampled point clouds. As shown in Fig. 8, the encoder is devised to perform point-wise feature extraction on the subsampled point cloud, and the upsampling decoder is designed to reconstruct the original dense point cloud with offset attention (Guo et al., 2021) to refine global shape structure.

Liu, Liu et al. (2022) proposed a coarse-to-fine reconstruction framework, dubbed SPU-Net, integrating self-attention with graph convolution network (GCN) for contextual feature extraction and generating fine point sets with hierarchically learnable 2D grids. Zhao et al. (2021) introduced SSPU-Net by leveraging the shape coherence between input
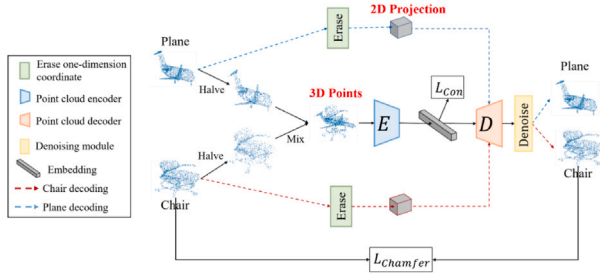
Fig. 9. The schematic of Mixing and Disentangling (MD) pretext. The two input point clouds are separately halved and mixed into a hybrid object feeding to the encoder E to mine the geometry-aware embedding. The 'Erase' operation is applied to obtain the 2D projection from both original input point clouds simultaneously. The instance-adaptive decoder D receives the embedding together with the two partial projections as input to disentangle the blended shape into the original two point clouds. The chamfer distance is used to measure the reconstruction error between generated point clouds and the original ones.
Source: This figure is adapted from Sun et al. (2022).

Fig. 10. Demonstration of shape self-correction pretext. The input point cloud is firstly preprocessed by a shape-disorganizing module to generate a deformed point cloud and then fed to the encoder to learn the geometry-aware representation. Two separate task heads are constructed to distinguish and segment points belonging to distorted parts, and subsequently reconstruct the partial-deformed objects. The well-trained feature extractor is transferred to downstream tasks to estimate the feature capturing capability.
Source: This figure is adapted from Chen et al. (2021).

sparse and generated dense point clouds. In addition, it has an image-consistent loss among multi-view rendered images to capture the latent patterns of underlying point structures.

PUFA-GAN (Liu, Yuan et al., 2022), a frequency-aware framework, utilizes a graph filter to extract high frequency (HF) points of sharp edges and corners so that the discriminator could focus on the HF geometric properties and enforce the generator producing neat and more uniform upsampled point clouds. To get rid of the fixed upsampling factor restriction, Zhao, Liu et al. (2022) presented a self-supervised arbitrary-scale (SSAS) framework with a magnification-flexible upsampling strategy. Instead of direct mapping from sparse to dense point clouds, the proposed scheme seeks the nearest projection points on the implicit surface for seed points via two functions, which are exploited to estimate the projection direction and distance, respectively.

3.1.4. Disentanglement

Models pre-trained under the SSL paradigm usually tend to learn well the low-level geometric features of point clouds, such as pose, contour, and shape information, but overlook the high-level semantic content understanding, which often leads to unsatisfactory performance in downstream tasks such as object classification that requires global discriminative capability. To tackle this issue, disentanglement-based SSL pretexts are proposed to separate the low-level geometric features from the high-level semantic embedding. Feature extraction is performed based on various contents using distinct modules to obtain hierarchical representations.

Tsai et al. (2022) proposed a disentanglement framework that uncouples content and pose attributes in partial point clouds to enhance both geometric and semantic feature abstraction. Two encoders are employed to learn the content and multi-view poses separately, where the gained pose representation should predict the viewing angle and navigate the partial point cloud reconstruction cooperated with the content from another specific view. Likewise, Xu et al. (2022) presented a universal Contour-Perturbed Reconstruction Network (CP-Net) that disentangles a point cloud into contour and content ingredients. A concise contour-perturbed augmentation unit is exploited on the contour component and retains the content part of the point cloud. Therefore, the self-supervisor is able to concatenate the content component for advanced semantic comprehension.

Different from the above two pretexts, Mixing and Disentangling (MD) (Sun et al., 2022) blends two disparate point shapes into a hybrid object and attains geometry-aware embedding from the encoder. An instance-adaptive decoder is then leveraged to restore the original geometries based on the obtained embedding by disentangling the mixed shape. As shown in Fig. 9, except for the main encoder–decoder structure, the proposed scheme also encompasses a coordinate
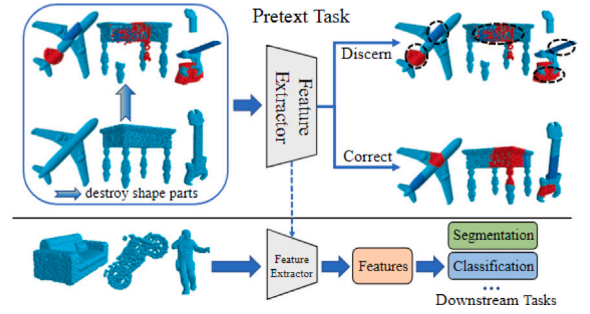
extracting operation 'Erase', which randomly drops one-dimension coordinate of each point to provide an extra 2D partial projection to better reconstruct the original point cloud shapes.

3.1.5. Deformation reconstruction

Point cloud deformation is a common phenomenon in real-world data scanning, which is usually caused by object distortion, sensor noise, or external occlusion. It has been discovered that SSL by reconstructing the original point cloud from the artificially deformed one (e.g. adding Gaussian noise or local translation) enables the learned model to obtain geometric perception as well as context awareness.

Chen et al. (2021) proposed a shape self-correction pretext to mine implicit geometric embeddings of point clouds. The pretext assumes that a robust shape representation could identify and correct distorted regions of a shape. As shown in Fig. 10, the proposed scheme imposes destruction over certain regions by a shape-disorganizing module and sends the deformed point cloud to the feature extractor for embedding learning. Two task heads are built separately to discern the distorted components and further restore them to their original normal shapes for fine-grained geometric and contextual feature exploration.

Achituve et al. (2021) conducted the first study of SSL for domain adaptation (DA) on point cloud via Deformation Reconstruction (DefRec). By mapping the dislocating points to their original location, the model is able to obtain the latent statistical structure of the input point cloud. Moreover, the distribution gap between source and target domains is bridged by the learned representation since they are invariant to distribution shift.

FoldingNet (Yang et al., 2018) presents a novel folding-based decoder to perform deformation on the canonical 2D grid to fit an arbitrary 3D object surface. Instead of deforming the point cloud, the folding operation exerts a virtual force induced by the embedding captured from input to stretch a 2D grid lattice to reproduce the 3D surface structure. This approach tackles issues caused by point cloud's irregular attributes by applying implicit 2D grid constraints. Based on the folding-based decoder, Chen et al. (2019) integrated graph topology inference and graph filtering modules into the decoder to learn pairwise relationships between 3D points and refine the coarse reconstruction. The superiority of graph smoothness (over spatial smoothness) as a prior to model 3D point clouds is utilized to further improve the reconstruction quality and consequently unsupervised performance.

3.1.6. Generation and discrimination

The generation and discrimination pretext is a unique paradigm that designs a discriminator module to distinguish whether the fed point cloud is reconstructed from noise distribution or truly sampled. During

Table 3
Summary of contrast-based point cloud SSL methods.

| Year	Method	Sub-categories	Contributions
2020	Info3D (Sanghi, 2020)	Object contrast	Maximizing mutual information between objects and their transformations
2022	AFSRL (Lu, Dai, Li, & Su, 2022)	Object contrast	Imposing data-level augmentation and feature enhancement simultaneously
2019	Contrasting and clustering (Zhang & Zhu, 2019)	Object contrast	Solving part contrast and object cluster tasks consecutively
2021	Hard negatives (Du, Gao, Hu, & Li, 2021)	Object contrast	Leveraging self-similar point cloud patches; facilitating hierarchical context primitives capturing
2020	PointContrast (Xie et al., 2020)	Scene contrast	Obtaining dense features at point-level on complex scenes by point contrast
2021	Contrastive Scene Contexts (Hou, Graham, Nießner, & Xie, 2021)	Scene contrast	Introducing ShapeContext local descriptor and achieving data-efficiency
2021	CoCoNets (Lal, Prabhudesai, Mediratta, Harley, & Fragkiadaki, 2021)	Scene contrast	Mapping RGB-D images to 3D points by optimizing view-contrastive prediction
2020	P4Contrast (Liu et al., 2020)	Scene contrast	Utilizing synergies between two modalities for better feature extraction
2021	DepthConstrast (Zhang, Girdhar, Joulin, & Misra, 2021)	Scene contrast	Applying Instance Discrimination on depth maps
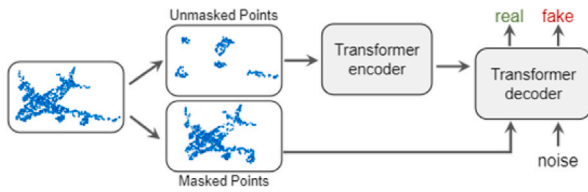
Fig. 11. The general pipeline of the Mask-Point model. The reconstruction challenge is formulated as a discriminative pretext to determine whether the source of the extracted sample is a masked point cloud or a random noise.
Source: The figure is adapted from Liu, Cai et al. (2022).

Fig. 12. Illustration of a self-contrastive paradigm. Patch A is selected as the anchor and the symmetrical part Patch D is the positive sample. Patch B and C are the negative samples, where Patch B is hard to distinguish due to its comparative similarity to the anchor.
Source: The figure is adapted from Du et al. (2021).

the adversarial training process, the generator (encoder) and discriminator (decoder) compete with each other and are updated alternatively so that both components can be transferred for downstream tasks.

PC-GAN (Li et al., 2018) is specifically designed for point clouds and employs a hierarchical and interpretable sampling strategy inspired by Bayesian and implicit generative models to tackle the issue of missing constraints on the discriminator. Sarmad et al. (2019) introduced a reinforcement learning (RL) agent to control the GAN to extract implicit representations from noisy and partial input to generate high-fidelity and entire point clouds. Meanwhile, applying an RL agent to seek the best-fit input of GAN to produce low-dimensional latent embedding relieves the challenge of unstable GAN training. Shu et al. (2019) introduced a tree-structured graph convolutional network (TreeGCN) as the generator, leveraging ancestor information to boost the representation of the point. It is more efficient in computation than using neighborhood features as adopted in regular GCNs. PU-GAN (Li et al., 2019) and PUFA-GAN (Liu, Yuan et al., 2022), both employed GANs-based models to generate dense and uniform point clouds with innovative modules for feature aggregation enhancement and high-frequency point filtering.

Liu, Cai et al. (2022) proposed a discriminative mask pre-training transformer framework, MaskPoint, which combines mask and discrimination techniques to perform simple binary classification between masked object points and sampled noise. As shown in Fig. 11, the original complete point cloud is divided into 90% masking portion and a 10% visible portion. Two kinds of query, where the real is sampled from masked point clouds while the fake is derived from random noise, are fed to the decoder for classification. During the discrimination process, the model is required to deduce the full geometry from small visible portions.

3.1.7. Summary for reconstruction-based methods

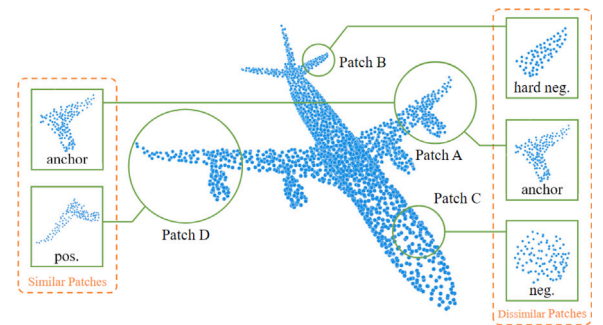Reconstruction-based methods have been the most prevalent ones in SSL in recent years. The pre-trained models can learn more fine-grained regional features through the reconstruction process and build semantic relationships between distinct pieces and overall point objects. MaskSurf (Zhang, Lin, He et al., 2022) achieves the state-of-the-art performance in downstream tasks such as object classification and part segmentation. 3D jigsaw (Sauder & Sievers, 2019b) can capture spatial information via rearranging randomly disordered patches. Nevertheless, the reconstruction process usually requires expensive computation and memory resources with point-wise operations on thousands of points.

3.2. Contrast-based methods

Contrastive learning is a popular mode of SSL that encourages augmentation of the same input to have more comparable representations. The general approach is to expand the views of input point clouds (anchors) by various data augmentation techniques. In particular, it tries to enforce positive samples augmented from the same anchor more similar than negative samples from different anchors in the feature space. In this section, we will introduce contrast-based methods with representative examples and discuss their contributions and limitations. A brief summary of these methods is shown in Table 3.

3.2.1. Object contrast

Traditional contrastive learning research usually focuses on instance-wise objects. The priority is on overall semantic learning through discriminative pretext tasks that capture context similarity and difference of point clouds. Such an object-contrast paradigm performs data augmentation on relatively large patches or whole single point objects to capture global geometric awareness.
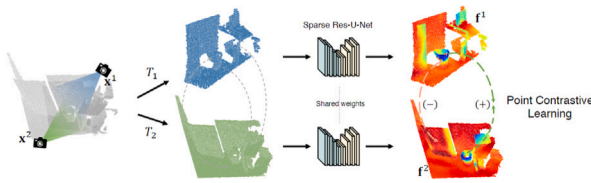
Fig. 13. The illustration of PointContrast. Contrast is performed at the point-level between two transformed point clouds, where positive samples are the matched points while negative samples are the unmatched points across two views.
Source: The figure is adapted from Xie et al. (2020).

Fig. 14. The schematic view of cross-modality and cross-view correspondences. The 3D point cloud objects and corresponding pairs of multi-view rendered images are sampled from the same mesh input, respectively. The relation of diverse views is captured as the supervision signal by sustaining the alignment among multi-view and cross-domain representations.
Source: The figure is adapted from Jing et al. (2021).

Sanghi (2020) proposed Info3D, which takes inspiration from Contrastive Predictive Coding (Oord, Li, & Vinyals, 2018) and Deep InfoMax (Velickovic et al., 2019), to obtain rotation-insensitive representation by maximizing mutual information between 3D objects and their local chunks as well as geometrically transformed versions. Lu et al. (2022) proposed the Augmentation Fusion Self-Supervised Representation Learning (AFSRL) framework, which imposes data-level augmentation and feature enhancement simultaneously to construct a stable and invariant point cloud embedding. The correspondence between augmented pairs is acquired, and the invariant semantic is maintained under perturbations during augmentation.

Zhang and Zhu (2019) introduced a simple two-phase unsupervised GCN framework (contrasting and clustering), to capture superior point embedding by solving part contrast and object cluster tasks consecutively. Du et al. (2021) presented a self-contrastive paradigm leveraging self-similar point cloud patches within a single point cloud to facilitate local shape and global context primitives capturing. As shown in Fig. 12, according to the nonlocal self-similar property of the point cloud, where regional geometry remains invariant after affine transformation, the self-similar point cloud patches are treated as positive samples otherwise negative based on the inferred similarity score. Moreover, hard negative samples, close to positive samples in the representation space, are sampled for more discriminative and expressive representation learning.

3.2.2. Scene contrast

Different from object-contrast, the scene-contrast paradigm concentrates on scenes to capture broader environmental context and neighborhood perception, which is more relevant to real-world complex scenarios.

To address the domain gap issue (i.e., it is insufficient to capture a global representation from object instances), Xie et al. (2020) proposed PointContrast, a sparse residual U-Net based framework aiming to obtain dense features at the point-level on complex scenes. As shown in Fig. 13, two views x^1 and x^2 are produced from a complicated point cloud scene, where corresponding pairs are computed between these two views as the positive samples. Two rigid transformations T^1 and T^2 are utilized to increase the difficulty of the pretext which demands the network to learn the invariant embedding under random geometric shift. The contrastive loss is defined to shorten the distance between the matched points and enlarge the distance of mismatched points of the two overlapping partial scans so that the pre-training model can capture local descriptions and be universally pertinent to various advanced 3D understanding downstream tasks.

However, PointContrast only considers point correspondence matching but ignored the spatial configurations and contexts in a scene, e.g., relative pose and distance, therefore confining its transferability and scalability. To address this issue, Hou et al. (2021) presented Contrastive Scene Contexts to fuse spatial information into pre-training objects by introducing ShapeContext local descriptor (Xie, Liu, Chen, & Tu, 2018) partitioning and performing contrastive learning in each region. The method improves the performance and data efficiency on
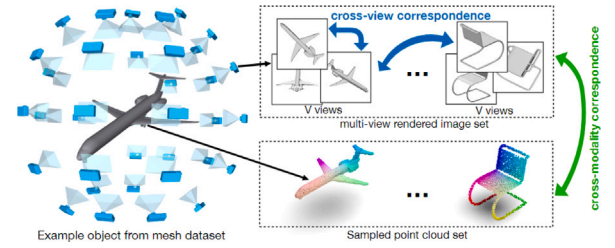
downstream tasks in which employing only 0.1% of point labels reaches the performance level with full supervision.

Continuous Contrastive 3D Networks (CoCoNets) (Lal et al., 2021) aims to infer latent scene representations by mapping RGB-D images to 3D point scenarios and optimizing view-contrastive prediction. P4Contrast (Liu et al., 2020), another RGB-D bi-modal SSL framework, proposes to contrast point-pixel pairs and provides additional flexibility for hard negative creation to exploit the synergies between two modalities for better feature extraction. DepthContrast (Zhang et al., 2021) circumvents the need for point correspondences and instead applies the Instance Discrimination (Wu et al., 2018) method on depth maps combined with a momentum encoder to improve the geometric perception.

3.2.3. Summary for contrast-based methods

Contrast-based SSL methods attempt to compare and grasp similarities and differences between point cloud samples, which is consistent with the way that humans usually learn. We introduced two types of subjects for contrast, object and scene, to show how this category of methods can learn geometric awareness from various perspectives. Some of these works, e.g. Hou et al. (2021), Lal et al. (2021) and Sanghi (2020), draw on the success in image processing and transfer it to the point cloud domain by adaptation. New data augmentation techniques are also proposed based on the discrete and irregular attributes of point clouds, which greatly enhance the feature extraction ability of the models. However, the representations captured for comparison always need a significant amount of memory, which is a considerable challenge for hardware requirements.

3.3. Alignment-based methods

Point cloud representation is generally invariant to transformations in terms of time flow, spatial motion, multi-view photography, etc. Based on this property, alignment-based methods have been proposed to learn the implicit embedding of point clouds by preserving the coherence of point features in spatiotemporal consistency, multi-view alignment, and multimodal fusion. A brief summary of the methods under this category is provided in Table 4.

3.3.1. Multi-view alignment

Compared to direct processing and feature extraction on 3D point clouds, projecting point clouds into 2D images for dimension reduction and utilizing mature image networks as well as 2D SSL technologies is relatively more accessible. To ensure that the learned embeddings sufficiently represent the entire 3D point cloud objects or scenes, multi-view alignment pretexts are necessary to preserve the integrity and uniformity of the point cloud features.

Info3D (Sanghi, 2020) aims to obtain rotation-insensitive representations by maximizing mutual information between 3D objects and

Table 4
Summary of alignment-based point cloud SSL methods.

Year	Method	Sub-categories	Contributions
2020	Info3D (Sanghi, 2020)	Multi-view alignment	Maximizing mutual information between objects and their transformations
2021	OcCo (Wang, Liu et al., 2021)	Multi-view alignment	Shielding and restoring occluded points in camera view
2021	Multi-view stereo (Yang, Alvarez, & Liu, 2021)	Multi-view alignment	Generating prime depth map as self-supervision signal
2021	Cross-view (Jing, Zhang, & Tian, 2021)	Multi-view alignment	Jointly learning both 3D point cloud and 2D image embedding concurrently
2022	Multi-view rendering (Tran, Hua, Tran, & Hoai, 2022)	Multi-view alignment	Encouraging 2D-3D global feature distributions to be similar
2022	Graph matching (Bian, Hui, Qian, & Xie, 2022)	Multi-view alignment	Exploring the local feature alignment between two domains
2021	Order prediction (Wang, Yang, Rong, Feng and Tian, 2021)	Spatiotemporal consistency	Sorting temporal order of sampled and disorganized point cloud clips
2021	STRL (Huang, Xie, Zhu, & Zhu, 2021)	Spatiotemporal consistency	Dual-branch network to predict representation of another temporally correlated input
2022	Futrue prediction (Mersch, Chen, Behley, & Stachniss, 2022)	Spatiotemporal consistency	Forecasting future point cloud scenes with lightweight model
2020	PointPainting (Vora, Lang, Helou, & Beijbom, 2020)	Multimodal fusion	Projecting LiDAR points into semantic segmentation diagram for traffic scenes
2021	PointAugmenting (Wang, Ma, Zhu and Yang, 2021)	Multimodal fusion	Replacing sub-optimal segmentation scores with high-dimension CNN features
2022	DeepFusion (Li et al., 2022)	Multimodal fusion	Exploiting cross-attention to capture long-range correlations of image-LiDAR pairs
2023	Open vocabulary 3D detection (Lu et al., 2023)	Multimodal fusion	Localize objects via connecting textual and point-cloud representations
2023	CLIP2 (Zeng et al., 2023)	Multimodal fusion	Constructing well-aligned instance-based text-image-point proxies from complex scenarios
2023	ULIP (Xue et al., 2023)	Multimodal fusion	Aligning a 3D embedding to pre-aligned image-text feature space to obtain unified representation

their local chunks for patch-level consistency. Occlusion Completion (OcCo) (Wang, Liu et al., 2021) combines the idea of mask recovery shielding and restoring occluded points in a camera view for better spatial and semantic properties comprehension. Similarly, Yang et al. (2021) introduced an SSL multi-view stereo structure generating prime depth map as pseudo-labels and refined such self-supervision from neighboring views as well as high-resolution images by multi-view depth fusion iteratively. Furthermore, the correspondence of pixel/point of the point clouds and the corresponding multi-view images are aligned for cross-modality consistency.

Jing et al. (2021) proposed a novel SSL framework leveraging cross-modality and cross-view correspondences to jointly learn both 3D point cloud and 2D image embedding concurrently. As shown in Fig. 14, point cloud objects and comparable pairs of multi-view rendered images are sampled from the same mesh input. In addition to 2D-3D consistency, the contrastive notion is adopted into cross-view alignment that shortens intra-object distance while maximizing inter-object discrepancy of distinct rendered images. Similarly, Tran et al. (2022) presented a dual-branch model not only agreeing upon fine-grained pixel-point local representation but also encouraging 2D-3D global feature distributions as approaching as possible by exploiting knowledge distillation.

The alignment idea can also be applied to domain adaptation. Bian et al. (2022) introduced a graph-based framework exploring the local feature alignment between two domains. Local representation graphs are constructed dynamically on both domains, and then the matching pairs are generated via optimal transport. In addition, considering the correlations between different categories' features, a category-guided contrastive loss is formulated to capture the discriminative information on the target domain.

3.3.2. Spatiotemporal consistency

Unlike previous methods, the spatiotemporal approach is more concerned with long-range spatial and temporal invariance before and after certain point cloud frames, which are 4D data (XYZ coordinate + temporal dimension), to capture intrinsic characteristics of dynamic sequences.
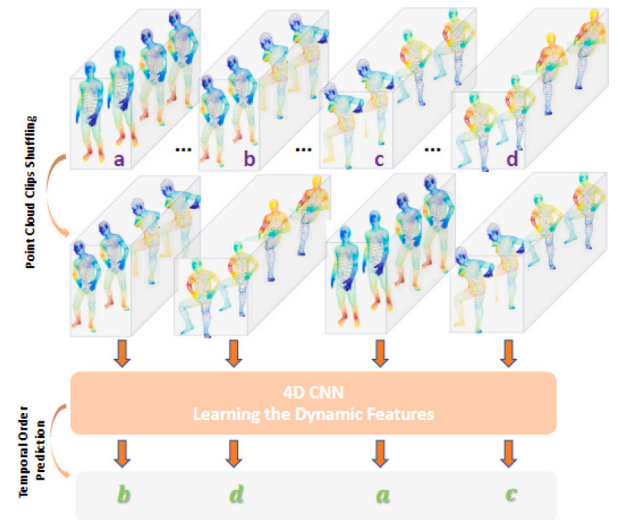
Fig. 15. Demonstration of point cloud sequence order prediction. The first row is the uniformly sampled point cloud clips from the continuous point cloud sequence. Then these clips are randomly shuffled and then fed into 4D CNN in the second row to learn the dynamic features of human actions, The original temporal order is predicted in a self-supervised manner.
Source: The figure is adapted from Wang, Yang et al. (2021).

Motivated by the success of Xu et al.'s work (Xu et al., 2019) in video SSL, Wang et al. proposed the first SSL scheme to gain effective temporal embeddings on dynamic point cloud data by sorting the temporal order of sampled and disorganized point cloud clips. As shown in Fig. 15, a few static point cloud frames are uniformly sampled and disordered, which are then processed by a 4D CNN to restore the disrupted fragments to the correct order on an unannotated, large-scale, sequential point cloud action recognition dataset.

Fig. 16. Demonstration of point decoration and deep fusion. (a) Previous cross-modal paradigms (Jing et al., 2021; Lal et al., 2021) decorate LiDAR points with camera feature on input-level for 3D detection. (b) DeepFusion (Li et al., 2022) fuses camera and LiDAR features extracted by respective encoders and leverages cross-attention consistency technique.
Source: The figure is adapted from Li et al. (2022).

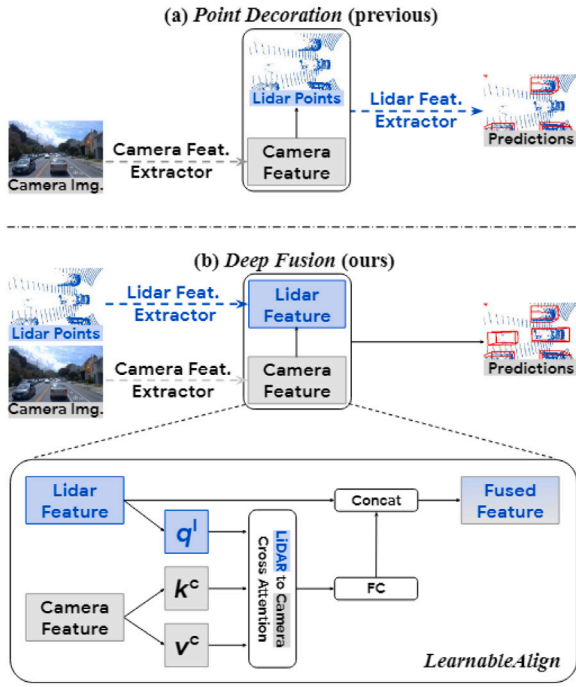Another spatiotemporal representation learning (STRL) (Huang et al., 2021) framework, inspired by BYOL (Grill et al., 2020), designs a dual-branch pipeline, referred to as online and target networks, to collaborate and promote each other. Specifically, the online network is enforced to predict the target network representation of another temporally correlated input, which is augmented by random spatial transformation, for spatiotemporal invariant contextual cues extraction. Taking training and inference time into account, Mersch et al. (2022) presented an innovative 3D spatiotemporal convolution encoder–decoder neural network consisting of fewer parameters to predict future point cloud scenes. Such a lightweight model concatenates range images as input to estimate forthcoming images and per-point scores in multiple future steps, so that spatial and temporal scene information can be captured simultaneously.

3.3.3. Multimodal fusion

Rather than simply requiring coherence between 2D-3D correspondences (Jing et al., 2021; Lal et al., 2021; Tran et al., 2022), automatic driving algorithms demand sophisticated collaboration between in-vehicle sensors. For example, cameras and LiDARs provide complementary information (e.g., colorful texture visualization and distance perception) for 3D object detection. Therefore, multimodal fusion is a promising direction to exploit the potential of images and point clouds for acquiring effective traffic scene features.

Li et al. (2022), Vora et al. (2020), and Wang, Ma et al. (2021) offered compact frameworks for tight sensor-fusion which could be implemented under the SSL paradigm without human annotations. PointPainting (Vora et al., 2020) is a sequential fusion method that projects LiDAR points onto semantic segmentation diagrams for traffic scenes with color marking. Each point is painted with a class score obtained from the image segmentation network and then can be utilized in any LiDAR detection approaches. Such a painting fusion method cleverly addresses the limitations of depth-blurring and scale ambiguity by consolidating the birds-eye and camera view.

PointAugmenting (Wang, Ma et al., 2021) adopts a late cross-modal fusion mechanism based on PointPainting, replacing the sub-optimal segmentation scores with high-dimension CNN features containing rich outlook hints and larger receptive fields to emphasize the delicate details. Moreover, a simple yet effective cross-modal data augmentation pastes virtual objects into images and point clouds for alignment between the camera and LiDAR. However, both PointPainting and PointAugmenting simply decorate LiDAR points with camera embeddings as shown in Fig. 16(a). To improve the performance on downstream tasks, DeepFusion (Li et al., 2022) proposed an end-to-end cross-modal fusion on the feature level, focusing on consistency improvement. As shown in Fig. 16(b), a block named LearnableAlign is introduced to exploit cross-attention to dynamically capture long-range correlations during the image-LiDAR fusion process to enhance the model's recognition and localization capability.

Natural language can also interact with image and point cloud data and be used for three-modalities fusion. Benefiting from vision-language pre-trained models, Lu et al. (2023) proposed an open-vocabulary 3D object detection framework without annotation. The detector can localize and classify objects by connecting text and point cloud representations using text prompting. To further explore the open-world 3D vision understanding, CLIP2 (Zeng et al., 2023) was introduced to construct well-aligned and instance-based text-image-point proxies from complex scenarios and boost the state-of-the-art performance on zero-shot and few-shot 3D recognition tasks by large margins. Likewise, ULIP (Xue et al., 2023), another text-image-point triplets pre-trained framework, was proposed to align a 3D embedding to pre-aligned image-text feature space to obtain unified representations. Therefore, this model enables cross-domain downstream tasks such as zero-shot 3D classification and image-to-point retrieval.

3.3.4. Summary for alignment-based methods

Alignment-based SSL methods utilize the inherent invariance of point clouds to learn the implicit embeddings for spatiotemporal consistency, multi-view alignment, and multimodal fusion. In multimodal fusion, bimodal (Li et al., 2022; Vora et al., 2020; Wang, Ma et al., 2021) or trimodal (Lu et al., 2023; Xue et al., 2023; Zeng et al., 2023) models take advantage of the complementary information of different modalities from various data sources. It is believed that multimodal fusion has a great potential in further automatic driving development. However, it also has to address the challenges of data conflicts among modalities as well as more suitable fusion solutions.

3.4. Motion-based methods

Various point cloud frames contain rich geometric patterns and kinematic schemas that are concealed in the movement of objects or scenes. The motion-based SSL paradigm focuses on dynamically capturing the intrinsic motion characteristics from spatial variations by taking advantage of traditional registration and scene flow estimation as pretexts. A brief summary on the methods under this category is shown in Table 5.

3.4.1. Registration

Point cloud registration is the task to merge two point clouds X and Y into a globally consistent coordinate system via estimating the rigid transformation matrix, which can be formulated as:

$$R, t = \underset{R \in SO(3), t \in \mathbb{R}^3}{\arg \min} \|\psi(RX + t) - \psi(Y)\|_2. \tag{5}$$

where $R \in SO(3)$ and $t \in \mathbb{R}^3$ indicate rotation matrix and translation vector, respectively; ψ is the feature extraction network learning the hierarchical informative features from dynamic point clouds. Unlike the classic ICP registration method (Besl & McKay, 1992) which iteratively searches correspondences and estimates rigid transformation, SSL registration can obtain informative point cloud features without high-quality ground-truth correspondences.

Table 5
Summary of motion-based point cloud SSL methods.

| Year	Method	Sub-categories	Contributions
2019	PRNet (Wang & Solomon, 2019)	Registration	Pioneer for partial-to-partial point cloud registration enabling coarse-to-fine refinement
2021	Part mobility (Shi, Cao, & Zhou, 2021)	Registration	Converting points to trajectories to derive the rigid transformation hypotheses
2022	SuperLine3D (Zhao et al., 2022)	Registration	Obtaining precise line representation under arbitrary scale perturbations
2022	DVD (Liu, Chen, Xu, Qiu and Chu, 2022)	Registration	Learning local and global point embedding jointly
2020	PointPWC-Net (Wu, Wang, Li, Liu, & Fuxin, 2020)	Scene flow estimation	Discretizing cost volume onto 3D point clouds in a coarse-to-fine fashion
2020	Just go with the flow (Mittal, Okorn, & Held, 2020)	Scene flow estimation	Optimizing two SSL losses based on nearest neighbors and cycle consistency
2021	Self-Point-Flow (Li, Lin, & Xie, 2021)	Scene flow estimation	Converting pseudo label matching problem as optimal transport task
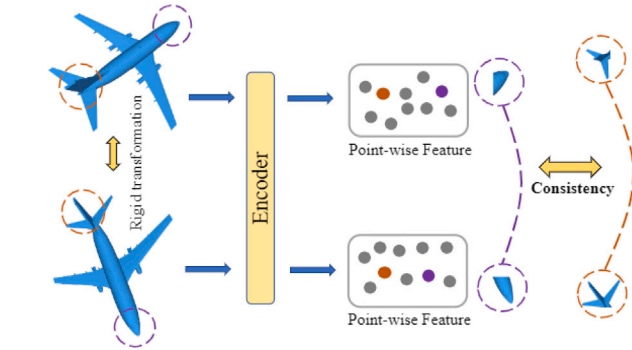
Fig. 17. Demonstration of deep versatile descriptors. The input consists of two point clouds before and after rigid transformations, where the common point components are utilized to train the encoder for global and local representation learning.
Source: The figure is adapted from Liu, Chen et al. (2022).

Fig. 18. Demonstration of just going with the flow. The nearest neighbor loss is utilized to push the predicted flow (green) close to the pseudo-ground truth (red) of the frame at $t + 1$. The cycle consistency loss is the penalty term to estimate the flow between predicted points (green) in the opposite direction to the original points (blue) in frame at t for temporal alignment.
Source: The figure is adapted from Mittal et al. (2020).

PRNet (Wang & Solomon, 2019) is a partial-to-partial registration method that enables coarse-to-fine refinement iteratively. Based on co-contextual information, the framework boils down the registration problem as a key point detection task, which aims to recognize the matching points from two input clouds. Shi (Wang & Solomon, 2019) presented a part mobility segmentation approach to understand the essential attributes of the dynamic object. Instead of directly processing the sequential point clouds, the raw input is converted to trajectories by point correspondence between successive frames to derive rigid transformation hypotheses. Analogously, Zhao, Yang et al. (2022) proposed an SSL line segmentation and description for LiDAR point clouds, called SuperLine3D, providing applicable line features for global registration without any prior hints. Compared to point embedding constrained by limited resolution, this segmentation model is capable of obtaining precise line representation under arbitrary scale perturbations.

Motivated by the observation that the local distinctive geometric structures of two subsets of point clouds can improve representations, Liu, Chen et al. (2022) introduced the deep versatile descriptors (DVDs) which learn local and global point embeddings jointly. As shown in Fig. 17, the co-occurring point cloud local regions, which retain the structural knowledge under rigid transformations, are regarded as the input of DVD to extract latent geometric patterns restrained by local consistency loss. To further enhance the model's capability of transformation awareness, reconstruction and normal estimation are added as auxiliary tasks for better alignment.

3.4.2. Scene flow estimation

Scene flow estimation is a vital computer vision task. For point clouds, its objective is to estimate the motion of objects by computing dense correspondences between consecutive LiDAR scans of a scene over time. The variation of points can be represented as 3D displacement vectors to describe the motions in terms of scene flow.

Wu et al. (2020) introduced the notion of cost volume and proposed a learnable point-based network called PointPWC-Net. The cost volume is discretized as input point pairs to reduce computational complexity;

additionally, an efficient upsampling strategy and wrap layers are employed. Mittal et al. (2020) proposed a novel SSL scene flow estimation network to achieve safe navigation during interactions with highly dynamic environments by optimizing two loss components based on the nearest neighbors and cycle consistency. As shown in Fig. 18, the nearest neighbor loss encourages the points predicted based on current moment t flowing toward occupied regions of the future frame at $t + 1$. The cycle consistency loss ensures that the points of the future frame $t + 1$ can be restored in the reverse direction back to frame t to avoid degenerate solutions by maintaining temporal consistency. Self-Point-Flow (Li et al., 2021) employs more than 3D point coordinates, surface normal, and color in one-to-one matching to generate pseudo labels and formulates the pseudo label generation issue as an optimal transport problem. It leverages a random walk module to refine annotation quality by imposing local alignment.

3.4.3. Summary for motion-based methods

Motion-based SSL methods learn elemental motion patterns from kinematic schemas and spatial variations of registration and scene flow estimation. Such works (Liu, Chen et al., 2022; Wang & Solomon, 2019; Wu et al., 2020) extracted the intrinsic dynamic characteristics by building the point-to-point correspondence between point clouds from forward and backward frames. However, it is found that the corresponding relationship is not guaranteed to be accurate, and sometimes spurious correspondences may lead to degenerating solutions and performance.

4. Downstream tasks

One of the primary objectives of SSL is to pre-train a backbone network and transfer it to solve the problems in downstream tasks.

Table 6

Summary of few-shot protocol performance of representative SSL methods on ModelNet40 (Wu et al., 2015) and ScanObjectNN (Uy et al., 2019). The results are reported in terms of OA (%).

Method	Backbone	5-way		10-way	
		10-shot	20-shot	10-shot	20-shot
ModelNet40					
Point-MAE (Pang et al., 2022)	Transformer	96.3	97.8	92.6	95.5
Point-BERT (Yu et al., 2021)	Transformer	94.6	96.3	91.0	92.7
OcCo (Wang, Liu et al., 2021)	PointNet	89.7	92.4	89.3	89.7
OcCo (Wang, Liu et al., 2021)	DGCNN	90.6	92.5	82.9	86.5
OcCo (Wang, Liu et al., 2021)	Transformer	94.0	95.9	89.4	92.4
3D jigsaw (Sauder & Sievers, 2019b)	PointNet	66.5	69.2	56.9	66.5
3D jigsaw (Sauder & Sievers, 2019b)	DGCNN	34.3	42.2	26.0	29.9
MaskSurf (Zhang, Lin, He et al., 2022)	Transformer	96.5	98.0	93.0	95.3
MaskPoint (Liu, Cai et al., 2022)	Transformer	95.0	97.2	91.4	93.4
ScanObjectNN					
Point-MAE (Pang et al., 2022)	Transformer	63.9	77.0	53.6	61.6
OcCo (Wang, Liu et al., 2021)	PointNet	70.4	72.2	54.8	61.8
OcCo (Wang, Liu et al., 2021)	DGCNN	72.4	77.2	57.0	61.6
3D jigsaw (Sauder & Sievers, 2019b)	PointNet	58.6	67.6	53.6	48.1
3D jigsaw (Sauder & Sievers, 2019b)	DGCNN	65.2	72.2	45.6	48.2
MaskSurf (Zhang, Lin, He et al., 2022)	Transformer	65.3	77.4	53.8	63.2

Therefore, performance of the model in downstream tasks could reflect the effectiveness of SSL to a certain degree. The evaluation criteria indicate whether the SSL methods can extract useful knowledge from pretext tasks with large-scale unlabeled point cloud data. In this section, we introduce four commonly used downstream tasks and provide the widely used evaluation metrics. In addition, we summarize and compare the performance of the aforementioned representative SSL methods in the corresponding downstream tasks.

4.1. Object classification

Object classification is a fundamental and prevalent downstream task that requires the model to output a most likely label for the given point cloud object to assess the overall semantic awareness of the pre-trained model. The two commonly used metrics for this task are Overall Accuracy (OA) and Mean Class Accuracy (mAcc). OA is the ratio of correctly classified objects to the total number of objects, and mAcc is the average of each class's accuracy. Object classification can be divided into three protocols based on task settings:

- **Few-shot:** Few-shot learning (FSL) is a challenging task that involves training with limited information provided by the downstream dataset. Specifically, the n-way, m-shot setting is employed, where n is the number of classes randomly selected from the dataset and m is the number of objects randomly sampled for each class. The trained model is evaluated on the test split. Few-shot protocol performance of reviewed SSL methods is shown in Table 6.
- **Fine-tuning:** The pre-trained feature extractor serves as the initial downstream backbone encoder, and the entire network is re-trained in a supervised manner with labels from the downstream datasets. Fine-tuning protocol performance of proposed SSL methods is presented in Table 7.
- **Linear classification:** The pre-trained feature extractor is frozen by stopping the backpropagation gradients. Linear classifiers are trained in a supervised manner with downstream datasets. Linear classification protocol performance of proposed SSL methods is shown in Table 8.

4.2. Part segmentation

Part segmentation is a fine-grained task that aims to distinguish and separate various components of an object, such as plane wings or desk legs. This task usually requires a model that can extract local point-level features more effectively than the overall discriminative ability required for object recognition. The popular evaluation criteria of point cloud part segmentation is the mean Intersection over Union (mIoU), which computes the ratio of the intersection of the predicted and ground truth part labels to the union of the two, across all categories ($mIoU_C$) or all instances ($mIoU_I$). Table 9 summarizes the results of part segmentation on the ShapeNetPart dataset based on SSL pre-training models and supervised fine-tuning in terms of $mIoU_C$ (%), $mIoU_I$ (%).

4.3. Semantic segmentation

Semantic segmentation requires a model to assign a semantic label to each points in the point cloud in order to group meaningful regions. It is frequently implemented on complicated outdoor or indoor scenes with background noise. mIoU, OA, and mAcc are commonly employed as estimation indicators to judge the feature extraction capability of pre-training models on the S3DIS dataset (Armeni et al., 2016), which contains six large-scale indoor venues, with the following two protocols. Performance of representative methods on semantic segmentation under the two protocols are shown in Table 10.

- **Area 5 test:** The SSL pre-trained model is fine-tuned on all areas except the largest area 5, which is chosen as the test set.
- **Six-fold cross validation:** Areas 1–6 are selected in turn as the test set and fine-tuned in the remaining 5 areas.

4.4. Object detection

Object detection is a task that involves localizing the 6 Degrees-of-Freedom (DoF) bounding box of an object and differentiating its category in a complex scene. The evaluation metric used is the Average Precision (AP), which measures the precision of the 3D bounding box at various recall levels. The threshold is usually set to 0.25 and 0.5. Table 11 summarizes the object detection performance of the SSL pre-training models on the SUN RGB-D (Song et al., 2015) and ScanNet (Dai et al., 2017) datasets.

5. Future directions

Although self-supervised learning has shown great success for point cloud processing, we have identified some of its deficiencies and limitations. We argue that SSL should not be studied in isolation but rather in conjunction with advanced techniques from other domains.

Table 7
Summary of fine-tuning protocol performance of representative SSL methods on ModelNet40 (Wu et al., 2015) and ScanObjectNN (Uy et al., 2019). ScanObjectNN has three challenges. The results are reported in terms of OA (%).

Method	Year	Pretext type	Backbone	Pre-train dataset	ModelNet40	ScanObjectNN OBJ-BG	OBJ-ONLY	PB-T50-RS
Supervised	2017	–	PointNet (Qi, Su et al., 2017)	–	89.2	73.3	79.2	68.0
	2017		PointNet++ (Qi, Yi et al., 2017)		90.7	82.3	84.3	77.9
	2019		DGCNN (Wang et al., 2019)		92.9	82.8	86.2	78.1
	2017		Transformer (Vaswani et al., 2017)		91.4	79.86	80.55	77.24
Point-MAE (Pang et al., 2022)	2022	Reconstruction	Transformer	ShapeNet	93.8	90.02	88.29	85.18
Point-BERT (Yu et al., 2021)	2021	Reconstruction	Transformer	ShapeNet	93.2	87.43	88.12	83.07
3D jigsaw (Sauder & Sievers, 2019b)	2019	Reconstruction	DGCNN	ShapeNet	92.4	82.0	82.1	–
MaskSurf (Zhang, Lin, He et al., 2022)	2022	Reconstruction	Transformer	ShapeNet	93.40	91.22	89.17	85.81
CloudContext (Sauder & Sievers, 2019a)	2019	Reconstruction	DGCNN	ShapeNet	90.8	–	–	–
UAE (Zhang, Shi et al., 2022)	2022	Reconstruction	DGCNN	ShapeNet	93.2	–	–	–
MD (Sun et al., 2022)	2022	Reconstruction	DGCNN	ModelNet40	93.39	–	–	–
Self-correction (Chen et al., 2021)	2021	Reconstruction	PointNet	ShapeNet	90.0	–	–	–
Self-correction (Chen et al., 2021)	2021	Reconstruction	RSCNN	ShapeNet	93.0	–	–	–
MaskPoint (Liu, Cai et al., 2022)	2022	Reconstruction	Transformer	ShapeNet	93.8	88.1	89.3	84.3
Info3D (Sanghi, 2020)	2020	Contrast	PointNet	ShapeNet	90.20	–	–	–
Info3D (Sanghi, 2020)	2020	Contrast	DGCNN	ShapeNet	93.03	–	–	–
OcCo (Wang, Liu et al., 2021)	2021	Alignment	PointNet	ModelNet40	90.1	–	–	–
OcCo (Wang, Liu et al., 2021)	2021	Alignment	DGCNN	ModelNet40	93.0	82.1	83.2	–
Cross-view (Jing et al., 2021)	2021	Alignment	DGCNN	ModelNet40	93.0	82.2	83.0	–
Multi-view rendering (Tran et al., 2022)	2022	Alignment	PointNet	ModelNet40	89.5	78.5	80.5	–
Multi-view rendering (Tran et al., 2022)	2022	Alignment	DGCNN	ModelNet40	93.2	84.5	84.3	–
STRL (Huang et al., 2021)	2021	Alignment	DGCNN	ShapeNet	93.1	–	–	–
ULIP (Xue et al., 2023)	2023	Alignment	PointMLP	–	94.7	–	–	–

In this section, we discuss a number of future research directions that have the potential to improve the SSL learning capability and performance on downstream tasks, in combinations with the prevailing views from Shao, Zhao, Yuan, Ding, and Wang (2022).

5.1. Few-shot and zero-shot learning

There have been a good number of publicly available, labeled datasets for SSL research. However, real scenarios often face the data shortage or quality challenges, such as damaged labels, missing information, and uneven assortment. Few-shot learning (FSL) (Garcia & Bruna, 2017) is considered as a potential solution that allows the network to train under the situations with very small amount of data. It is also possible to identify new sample types that have not been seen before in a test task without training samples. This method is often referred to as the zero-shot learning (ZSL). Both SSL and FSL (ZSL) (Romera-Paredes & Torr, 2015) can free models from the reliance on large annotated datasets and reduce the cost. In addition, the combination of these two could potentially improve the generalization capability the models.

5.2. Multiple modality interaction and fusion

Despite of the assorted modalities in many existing datasets, for example, for outdoor autonomous driving (Caesar et al., 2020; Geiger et al., 2012; Sun et al., 2020), researchers normally only focus on and make use of the point cloud data while ignoring the connections and alignment relationships with data of other modalities. We have seen some recent research works design models (Li et al., 2022; Vora et al., 2020; Wang, Ma et al., 2021) for multi-model data alignment and fusion, primarily point clouds and images. We anticipate more research to focus on cross-modal SSL with more diverse modalities, e.g., natural language, radar and voice, exploiting the unique characteristics of each modality and the synergy among them to build transportation systems, e.g. autonomous driving and traffic scene analysis, with more artificial general intelligence.

5.3. Hierarchical feature extraction

To cope with sophisticated downstream tasks with somehow conflicting objectives, for example, object classification which requires overall semantic understanding and part segmentation which requires fine-grained geometrical awareness, SSL models should have the capability for both global perception and local analysis. This necessitates hierarchical feature extraction; in particular, interactions between feature representations on different levels in the hierarchy need to be considered to discover the implicit relations. Therefore, we suggest that hierarchical feature extraction should be embedded in the SSL paradigm to improve the model's capability to capture both global and local features from point clouds.

Table 8

Summary of linear classification protocol performance of representative SSL methods on ModelNet10/40 (Wu et al., 2015). The results are reported in terms of OA (%).

Method	Pretext type	Backbone	ModelNet10/40
Point-MAE (Pang et al., 2022)	Reconstruction	Transformer	–/91.41
Orientation estimation (Poursaeed et al., 2020)	Reconstruction	PointNet	–/88.6
Orientation estimation (Poursaeed et al., 2020)	Reconstruction	DGCNN	–/90.75
3D jigsaw (Sauder & Sievers, 2019b)	Reconstruction	PointNet	91.61/87.31
3D jigsaw (Sauder & Sievers, 2019b)	Reconstruction	DGCNN	94.52/90.64
Graph topology (Chen et al., 2019)	Reconstruction	DGCNN	95.93/89.55
MaskSurf (Zhang, Lin, He et al., 2022)	Reconstruction	Transformer	–/92.26
CloudContext (Sauder & Sievers, 2019a)	Reconstruction	DGCNN	94.5/89.3
UAE (Zhang, Shi et al., 2022)	Reconstruction	DGCNN	95.6/92.9
Pose Disentanglement (Tsai et al., 2022)	Reconstruction	PointNet	–/90.1
Pose Disentanglement (Tsai et al., 2022)	Reconstruction	DGCNN	–/92.0
CP-Net (Xu et al., 2022)	Reconstruction	RSCNN	–/91.9
FoldingNet (Yang et al., 2018)	Reconstruction	GNN	94.4/88.4
Self-correction (Chen et al., 2021)	Reconstruction	PointNet	93.3/89.9
Self-correction (Chen et al., 2021)	Reconstruction	RSCNN	95.0/92.4
PC-GAN (Li et al., 2018)	Reconstruction	GAN	–/87.5
Info3D (Sanghi, 2020)	Contrast	PointNet	–/89.8
Info3D (Sanghi, 2020)	Contrast	DGCNN	–/91.6
AFSRL (Lu et al., 2022)	Contrast	GNN	–/91.5
Contrasting and clustering (Zhang & Zhu, 2019)	Contrast	DGCNN	93.8/86.8
Hard negatives (Du et al., 2021)	Contrast	DGCNN	–/89.6
OcCo (Wang, Liu et al., 2021)	Alignment	DGCNN	–/89.2
Cross-view (Jing et al., 2021)	Alignment	GNN	–/89.8
Multi-view rendering (Tran et al., 2022)	Alignment	PointNet	–/89.7
Multi-view rendering (Tran et al., 2022)	Alignment	DGCNN	–/91.7
STRL (Huang et al., 2021)	Alignment	PointNet	–/88.3
STRL (Huang et al., 2021)	Alignment	DGCNN	–/90.9
PRNet (Wang & Solomon, 2019)	Motion	DGCNN	–/85.2

Table 9

Summary of performance of representative methods on part segmentation using ShapeNetPart (Armeni et al., 2016).

Method	Type	Backbone	mIoU$_C$	mIoU$_I$
Supervised	–	PointNet (Qi, Su et al., 2017)	83.39	83.7
		PointNet++ (Qi, Yi et al., 2017)	81.85	85.1
		DGCNN (Wang et al., 2019)	82.33	85.2
		Transformer (Vaswani et al., 2017)	83.42	85.1
Point-MAE (Pang et al., 2022)	Reconstruction	Transformer	84.19	86.1
Point-BERT (Yu et al., 2021)	Reconstruction	Transformer	84.11	85.6
3D jigsaw (Sauder & Sievers, 2019b)	Reconstruction	PointNet	–	82.2
3D jigsaw (Sauder & Sievers, 2019b)	Reconstruction	DGCNN	–	85.3
MaskSurf (Zhang, Lin, He et al., 2022)	Reconstruction	Transformer	84.36	86.1
CloudContext (Sauder & Sievers, 2019a)	Reconstruction	DGCNN	–	81.5
UAE (Zhang, Shi et al., 2022)	Reconstruction	DGCNN	–	85.6
Pose Disentanglement (Tsai et al., 2022)	Reconstruction	PointNet	–/83.8	
Pose Disentanglement (Tsai et al., 2022)	Reconstruction	DGCNN	–/85.1	
MD (Sun et al., 2022)	Reconstruction	DGCNN	–	85.5
Self-correction (Chen et al., 2021)	Reconstruction	PointNet	–	84.1
Self-correction (Chen et al., 2021)	Reconstruction	RSCNN	–	85.2
MaskPoint (Liu, Cai et al., 2022)	Reconstruction	Transformer	84.4	86.0
AFSRL (Lu et al., 2022)	Contrast	GNN	–/85.7	
Hard negatives (Du et al., 2021)	Contrast	DGCNN	–/82.3	
PointContrast (Xie et al., 2020)	Contrast	U-Net	–	85.1
OcCo (Wang, Liu et al., 2021)	Alignment	PointNet	–	83.4
OcCo (Wang, Liu et al., 2021)	Alignment	DGCNN	–	85.0
Cross-view (Jing et al., 2021)	Alignment	DGCNN	79.1	83.7
Multi-view rendering (Tran et al., 2022)	Alignment	PointNet	–	83.3
Multi-view rendering (Tran et al., 2022)	Alignment	DGCNN	–	84.7
PRNet (Wang & Solomon, 2019)	Motion	DGCNN	78.8/82.5	

5.4. Multiple tasks pre-training

Up to now, most point cloud SSL methods have only one specific pre-training pretext while few works train diverse tasks concurrently. The main resistance is that multi-tasking has to consider the compatibility and synergy between various pretexts simultaneously, and fit each loss item for steady parameter updating. This is also one of the very reasons why a model performs well on one downstream task but not others. Indeed, distinct proxies could provide useful information from various perspectives of point clouds so that jointly training multiple tasks could facilitate the network to learn more comprehensive representations; obviously, more research on multi-task SSL is needed to push the research one step further.

5.5. Theory and interpretability

Similar to traditional deep learning, point cloud SSL lacks sufficient theoretical support and has poor interpretation. The process of model

Table 10

Summary of performance of representative methods on semantic segmentation using S3DIS (Armeni et al., 2016).

Method	Type	Backbone	OA	mAcc	mIoU
Supervised	–	PointNet (Qi, Su et al., 2017)	78.6	49.0	47.7
		DGCNN (Wang et al., 2019)	84.1	–	56.1
		Transformer (Vaswani et al., 2017)	86.8	68.6	60.0
Area 5 test					
Point-MAE (Pang et al., 2022)	Reconstruction	Transformer	87.4	69.4	61.0
OcCo (Wang, Liu et al., 2021)	Alignment	PointNet	–	83.6	44.5
OcCo (Wang, Liu et al., 2021)	Alignment	DGCNN	–	87.0	49.5
3D jigsaw (Sauder & Sievers, 2019b)	Reconstruction	PointNet	–	82.5	43.6
3D jigsaw (Sauder & Sievers, 2019b)	Reconstruction	DGCNN	–	86.8	48.2
MaskSurf (Zhang, Lin, He et al., 2022)	Reconstruction	Transformer	88.3	69.9	61.6
PointContrast (Xie et al., 2020)	Contrast	SR-UNet	–	77.0	70.9
Contrastive Scene Contexts (Hou et al., 2021)	Contrast	DGCNN	–	–	73.8
DepthConstrast (Zhang et al., 2021)	Contrast	PointNet++	–	72.1	64.8
Multi-view rendering (Tran et al., 2022)	Alignment	PointNet	–	85.0	46.7
Multi-view rendering (Tran et al., 2022)	Alignment	DGCNN	–	87.0	49.9
Six-fold cross validation					
OcCo (Wang, Liu et al., 2021)	Alignment	PointNet	82.0	–	54.9
OcCo (Wang, Liu et al., 2021)	Alignment	DGCNN	84.6	–	58.0
3D jigsaw (Sauder & Sievers, 2019b)	Reconstruction	PointNet	80.1	–	52.6
3D jigsaw (Sauder & Sievers, 2019b)	Reconstruction	DGCNN	84.1	–	55.6
CloudContext (Sauder & Sievers, 2019a)	Reconstruction	DGCNN	78.9	–	47.6
Multi-view rendering (Tran et al., 2022)	Alignment	PointNet	–	83.2	52.1
Multi-view rendering (Tran et al., 2022)	Alignment	DGCNN	–	87.5	59.0

Table 11

Summary of performance of representative methods on object detection using SUN RGB-D (Song et al., 2015) and ScanNet (Dai et al., 2017). The pre-training input only contains the point cloud geometry.

Method	Type	Backbone	SUN RGB-D		ScanNet	
			AP_{25}	AP_{50}	AP_{25}	AP_{50}
Point-BERT (Yu et al., 2021)	Reconstruction	Transformer	–	–	61.0	38.3
MaskPoint (Liu, Cai et al., 2022)	Reconstruction	Transformer	–	–	64.2	42.0
PointContrast (Xie et al., 2020)	Contrast	SR-UNet	57.5	34.8	59.2	38.0
PointContrast (Xie et al., 2020)	Contrast	VoteNet	59.2	38.0	57.5	34.8
DepthConst (Zhang et al., 2021)	Contrast	PointNet++	–	–	61.3	–
DepthConst (Zhang et al., 2021)	Contrast	VoteNet	64.0	42.9	61.6	35.5
DepthConst (Zhang et al., 2021)	Contrast	H3DNet	69.0	50.0	63.5	43.4
Multi-view rendering (Tran et al., 2022)	Alignment	DGCNN	58.1	35.1	60.3	39.2
STRL (Huang et al., 2021)	Alignment	VoteNet	58.2	–	–	–

training is conducted as a black-box, making it difficult for human users to analyze the results. Most of the technical works demonstrate their contributions via ablation studies and draw conclusions empirically. Such 'tried and tested' methods do not have theoretical support and are therefore difficult to verify, generalize and replicate. We suggest that future studies should include more inquiries into explainable theory, for example, the well-established theories from mutual information (Sayed, Brattoli, & Ommer, 2018) or causal inference (Wang et al., 2022), which can be applied in the design of network structures and loss functions.

6. Conclusion

Point cloud self-supervised learning fundamentally moves away from models' dependency on manual annotations. The learning paradigm focuses on the design of pre-training pretext tasks to enable the models to extract effective features and achieves performance competitive to the supervised learning paradigms in many downstream tasks. This paper extensively surveys recent representative deep neural network-based methods for self-supervised learning from point cloud data. A novel taxonomy is proposed to systematically classify the current research, especially the works publishes in the recent three years. Besides detailed analysis on the representative methods, we provide summaries on the commonly used datasets and performance comparison to make the survey more comprehensive. Future research directions are also discussed to hopefully provide an insightful view on the issues that the research community should pay attention to.

We hope that our work provides a valuable reference on point cloud SSL research and could motivate researchers to further explore this promising topic.

CRediT authorship contribution statement

Changyu Zeng: Conceptualization, Methodology, Data curation, Writing – original draft. **Wei Wang:** Writing – review & editing, Supervision, Project administration. **Anh Nguyen:** Supervision, Project administration. **Jimin Xiao:** Supervision, Project administration. **Yutao Yue:** Supervision, Project administration, Funding acquisition.

Declaration of competing interest

The authors declare the following financial interests/personal relationships which may be considered as potential competing interests: Yutao Yue reports financial support was provided by Wuxi National Hi-Tech District (WND). Yutao Yue reports financial support was provided by Jiangsu Industrial Technology Research Institute (JITRI).

Data availability

No data was used for the research described in the article.

References

Achituve, I., Maron, H., & Chechik, G. (2021). Self-supervised learning for domain adaptation on point clouds. In *Proceedings of the IEEE/CVF winter conference on applications of computer vision* (pp. 123–133).

Afham, M., Dissanayake, I., Dissanayake, D., Dharmasiri, A., Thilakarathna, K., & Rodrigo, R. (2022). Crosspoint: Self-supervised cross-modal contrastive learning for 3d point cloud understanding. In *Proceedings of the IEEE/CVF conference on computer vision and pattern recognition* (pp. 9902–9912).

Agrawal, P., Carreira, J., & Malik, J. (2015). Learning to see by moving. In *Proceedings of the IEEE international conference on computer vision* (pp. 37–45).

Arandjelovic, R., & Zisserman, A. (2017). Look, listen and learn. In *Proceedings of the IEEE international conference on computer vision* (pp. 609–617).

Armeni, I., Sener, O., Zamir, A. R., Jiang, H., Brilakis, I., Fischer, M., et al. (2016). 3D semantic parsing of large-scale indoor spaces. In *Proceedings of the IEEE conference on computer vision and pattern recognition* (pp. 1534–1543).

Besl, P. J., & McKay, N. D. (1992). Method for registration of 3-D shapes. In *Sensor fusion IV: Control paradigms and data structures, Vol. 1611* (pp. 586–606). Spie.

Bian, Y., Hui, L., Qian, J., & Xie, J. (2022). Unsupervised domain adaptation for point cloud semantic segmentation via graph matching. In *2022 IEEE/RSJ international conference on intelligent robots and systems (IROS)* (pp. 9899–9904). IEEE.

Caesar, H., Bankiti, V., Lang, A. H., Vora, S., Liong, V. E., Xu, Q., et al. (2020). nuscenes: A multimodal dataset for autonomous driving. In *Proceedings of the IEEE/CVF conference on computer vision and pattern recognition* (pp. 11621–11631).

Cai, X., Huang, C., Xia, L., & Ren, X. (2023). LightGCL: Simple yet effective graph contrastive learning for recommendation. arXiv preprint arXiv:2302.08191.

Caron, M., Misra, I., Mairal, J., Goyal, P., Bojanowski, P., & Joulin, A. (2020). Unsupervised learning of visual features by contrasting cluster assignments. *Advances in Neural Information Processing Systems, 33*, 9912–9924.

Chang, A. X., Funkhouser, T., Guibas, L., Hanrahan, P., Huang, Q., Li, Z., et al. (2015). Shapenet: An information-rich 3d model repository. arXiv preprint arXiv: 1512.03012.

Chen, S., Duan, C., Yang, Y., Li, D., Feng, C., & Tian, D. (2019). Deep unsupervised learning of 3D point clouds via graph topology inference and filtering. *IEEE Transactions on Image Processing, 29*, 3183–3198.

Chen, M., Hu, Q., Hugues, T., Feng, A., Hou, Y., McCullough, K., et al. (2022). STPLS3D: A large-scale synthetic and real aerial photogrammetry 3D point cloud dataset. arXiv preprint arXiv:2203.09065.

Chen, T., Kornblith, S., Norouzi, M., & Hinton, G. (2020). A simple framework for contrastive learning of visual representations. In *International conference on machine learning* (pp. 1597–1607). PMLR.

Chen, Y., Liu, J., Ni, B., Wang, H., Yang, J., Liu, N., et al. (2021). Shape self-correction for unsupervised point cloud understanding. In *Proceedings of the IEEE/CVF international conference on computer vision* (pp. 8382–8391).

Croitoru, I., Bogolin, S.-V., & Leordeanu, M. (2017). Unsupervised learning from video to detect foreground objects in single images. In *Proceedings of the IEEE international conference on computer vision* (pp. 4335–4343).

Csurka, G. (2017). Domain adaptation for visual applications: A comprehensive survey. arXiv preprint arXiv:1702.05374.

Dai, A., Chang, A. X., Savva, M., Halber, M., Funkhouser, T., & Nießner, M. (2017). Scannet: Richly-annotated 3d reconstructions of indoor scenes. In *Proceedings of the IEEE conference on computer vision and pattern recognition* (pp. 5828–5839).

Devlin, J., Chang, M.-W., Lee, K., & Toutanova, K. (2018). Bert: Pre-training of deep bidirectional transformers for language understanding. arXiv preprint arXiv: 1810.04805.

Doersch, C., Gupta, A., & Efros, A. A. (2015). Unsupervised visual representation learning by context prediction. In *Proceedings of the IEEE international conference on computer vision* (pp. 1422–1430).

Du, B., Gao, X., Hu, W., & Li, X. (2021). Self-contrastive learning with hard negative sampling for self-supervised point cloud learning. In *Proceedings of the 29th ACM international conference on multimedia* (pp. 3133–3142).

Ericsson, L., Gouk, H., & Hospedales, T. M. (2021). How well do self-supervised models transfer? In *Proceedings of the IEEE/CVF conference on computer vision and pattern recognition* (pp. 5414–5423).

Everingham, M., Van Gool, L., Williams, C. K. I., Winn, J., & Zisserman, A. The PASCAL Visual Object Classes Challenge 2012 (VOC2012) Results. http://www.pascal-network.org/challenges/VOC/voc2012/workshop/index.html.

Faktor, A., & Irani, M. (2014). Video segmentation by non-local consensus voting. In *BMVC* (p. 8).

Floridi, L., & Chiriatti, M. (2020). GPT-3: Its nature, scope, limits, and consequences. *Minds and Machines, 30*, 681–694.

Fraser, D. A. S. (1976). *Probability and statistics: Theory and applications: Technical Report.*

Garcia, V., & Bruna, J. (2017). Few-shot learning with graph neural networks. arXiv preprint arXiv:1711.04043.

Geiger, A., Lenz, P., & Urtasun, R. (2012). Are we ready for autonomous driving? the kitti vision benchmark suite. In *2012 IEEE conference on computer vision and pattern recognition* (pp. 3354–3361). IEEE.

Gidaris, S., Singh, P., & Komodakis, N. (2018). Unsupervised representation learning by predicting image rotations. In *International conference on learning representations*.

Goodfellow, I., Pouget-Abadie, J., Mirza, M., Xu, B., Warde-Farley, D., Ozair, S., et al. (2014). Generative adversarial nets. *Advances in Neural Information Processing Systems, 27*.

Grill, J.-B., Strub, F., Altché, F., Tallec, C., Richemond, P., Buchatskaya, E., et al. (2020). Bootstrap your own latent-a new approach to self-supervised learning. *Advances in Neural Information Processing Systems, 33*, 21271–21284.

Guo, M.-H., Cai, J.-X., Liu, Z.-N., Mu, T.-J., Martin, R. R., & Hu, S.-M. (2021). Pct: Point cloud transformer. *Computational Visual Media, 7*(2), 187–199.

Hackel, T., Savinov, N., Ladicky, L., Wegner, J. D., Schindler, K., & Pollefeys, M. (2017). Semantic3d. net: A new large-scale point cloud classification benchmark. arXiv preprint arXiv:1704.03847.

He, K., Chen, X., Xie, S., Li, Y., Dollár, P., & Girshick, R. (2021). Masked autoencoders are scalable vision learners. arXiv preprint arXiv:2111.06377.

He, K., Fan, H., Wu, Y., Xie, S., & Girshick, R. (2020). Momentum contrast for unsupervised visual representation learning. In *Proceedings of the IEEE/CVF conference on computer vision and pattern recognition* (pp. 9729–9738).

Hess, G., Jaxing, J., Svensson, E., Hagerman, D., Petersson, C., & Svensson, L. (2022). Masked autoencoders for self-supervised learning on automotive point clouds. arXiv preprint arXiv:2207.00531.

Hou, J., Graham, B., Nießner, M., & Xie, S. (2021). Exploring data-efficient 3d scene understanding with contrastive scene contexts. In *Proceedings of the IEEE/CVF conference on computer vision and pattern recognition* (pp. 15587–15597).

Hu, Q., Yang, B., Khalid, S., Xiao, W., Trigoni, N., & Markham, A. (2021). Towards semantic segmentation of urban-scale 3D point clouds: A dataset, benchmarks and challenges. In *Proceedings of the IEEE/CVF conference on computer vision and pattern recognition* (pp. 4977–4987).

Hua, B.-S., Pham, Q.-H., Nguyen, D. T., Tran, M.-K., Yu, L.-F., & Yeung, S.-K. (2016). Scenenn: A scene meshes dataset with annotations. In *2016 fourth international conference on 3D vision (3DV)* (pp. 92–101). Ieee.

Huang, S., Xie, Y., Zhu, S.-C., & Zhu, Y. (2021). Spatio-temporal self-supervised representation learning for 3d point clouds. In *Proceedings of the IEEE/CVF international conference on computer vision* (pp. 6535–6545).

Jayaraman, D., & Grauman, K. (2015). Learning image representations tied to ego-motion. In *Proceedings of the IEEE international conference on computer vision* (pp. 1413–1421).

Jiang, H., Larsson, G., Shakhnarovich, M. M. G., & Learned-Miller, E. (2018). Self-supervised relative depth learning for urban scene understanding. In *Proceedings of the European conference on computer vision (ECCV)* (pp. 19–35).

Jing, L., & Tian, Y. (2020). Self-supervised visual feature learning with deep neural networks: A survey. *IEEE Transactions on Pattern Analysis and Machine Intelligence, 43*(11), 4037–4058.

Jing, L., Zhang, L., & Tian, Y. (2021). Self-supervised feature learning by cross-modality and cross-view correspondences. In *Proceedings of the IEEE/CVF conference on computer vision and pattern recognition* (pp. 1581–1591).

Kazerouni, I. A., Fitzgerald, L., Dooly, G., & Toal, D. (2022). A survey of state-of-the-art on visual SLAM. *Expert Systems with Applications, 205*, Article 117734.

Koch, S., Matveev, A., Jiang, Z., Williams, F., Artemov, A., Burnaev, E., et al. (2019). Abc: A big cad model dataset for geometric deep learning. In *Proceedings of the IEEE/CVF conference on computer vision and pattern recognition* (pp. 9601–9611).

Lal, S., Prabhudesai, M., Mediratta, I., Harley, A. W., & Fragkiadaki, K. (2021). CoCoNets: Continuous contrastive 3D scene representations. In *Proceedings of the IEEE/CVF conference on computer vision and pattern recognition* (pp. 12487–12496).

Lewis, M., Liu, Y., Goyal, N., Ghazvininejad, M., Mohamed, A., Levy, O., et al. (2019). Bart: Denoising sequence-to-sequence pre-training for natural language generation, translation, and comprehension. arXiv preprint arXiv:1910.13461.

Li, R., Li, X., Fu, C.-W., Cohen-Or, D., & Heng, P.-A. (2019). Pu-gan: a point cloud upsampling adversarial network. In *Proceedings of the IEEE/CVF international conference on computer vision* (pp. 7203–7212).

Li, R., Lin, G., & Xie, L. (2021). Self-point-flow: Self-supervised scene flow estimation from point clouds with optimal transport and random walk. In *Proceedings of the IEEE/CVF conference on computer vision and pattern recognition* (pp. 15577–15586).

Li, Y., Ma, L., Zhong, Z., Liu, F., Cao, D., Li, J., et al. (2020). Deep learning for LiDAR point clouds in autonomous driving: A review. *IEEE Transactions on Neural Networks*.

Li, Y., Yu, A. W., Meng, T., Caine, B., Ngiam, J., Peng, D., et al. (2022). Deepfusion: Lidar-camera deep fusion for multi-modal 3d object detection. In *Proceedings of the IEEE/CVF conference on computer vision and pattern recognition* (pp. 17182–17191).

Li, C.-L., Zaheer, M., Zhang, Y., Poczos, B., & Salakhutdinov, R. (2018). Point cloud gan. arXiv preprint arXiv:1810.05795.

Liu, H., Cai, M., & Lee, Y. J. (2022). Masked discrimination for self-supervised learning on point clouds. arXiv preprint arXiv:2203.11183.

Liu, D., Chen, C., Xu, C., Qiu, R., & Chu, L. (2022). Self-supervised point cloud registration with deep versatile descriptors. arXiv preprint arXiv:2201.10034.

Liu, X., Liu, X., Liu, Y.-S., & Han, Z. (2022). Spu-net: Self-supervised point cloud upsampling by coarse-to-fine reconstruction with self-projection optimization. *IEEE Transactions on Image Processing, 31*, 4213–4226.

Liu, Y., Yi, L., Zhang, S., Fan, Q., Funkhouser, T., & Dong, H. (2020). P4contrast: Contrastive learning with pairs of point-pixel pairs for RGB-D scene understanding. http://dx.doi.org/10.48550/arXiv.2012.13089, arXiv e-prints, arXiv:2012.13089, arXiv:2012.13089.

Liu, H., Yuan, H., Hou, J., Hamzaoui, R., & Gao, W. (2022). PUFA-GAN: A frequency-aware generative adversarial network for 3D point cloud upsampling. *IEEE Transactions on Image Processing, 31*, 7389–7402.

Lu, Z., Dai, Y., Li, W., & Su, Z. (2022). Joint data and feature augmentation for self-supervised representation learning on point clouds. arXiv preprint arXiv:2211.01184.

Lu, Y., Xu, C., Wei, X., Xie, X., Tomizuka, M., Keutzer, K., et al. (2023). Open-vocabulary point-cloud object detection without 3d annotation. In *Proceedings of the IEEE/CVF conference on computer vision and pattern recognition* (pp. 1190–1199).

Matti, D., Ekenel, H. K., & Thiran, J.-P. (2017). Combining LiDAR space clustering and convolutional neural networks for pedestrian detection. In *2017 14th IEEE international conference on advanced video and signal based surveillance (AVSS)* (pp. 1–6). http://dx.doi.org/10.1109/AVSS.2017.8078512.

Mersch, B., Chen, X., Behley, J., & Stachniss, C. (2022). Self-supervised point cloud prediction using 3D spatio-temporal convolutional networks. In *Conference on robot learning* (pp. 1444–1454). PMLR.

Mikolov, T., Chen, K., Corrado, G., & Dean, J. (2013). Efficient estimation of word representations in vector space. arXiv preprint arXiv:1301.3781.

Miller, G. A. (1995). WordNet: a lexical database for English. *Communications of the ACM, 38*(11), 39–41.

Min, C., Zhao, D., Xiao, L., Nie, Y., & Dai, B. (2022). Voxel-mae: Masked autoencoders for pre-training large-scale point clouds. arXiv preprint arXiv:2206.09900.

Mittal, H., Okorn, B., & Held, D. (2020). Just go with the flow: Self-supervised scene flow estimation. In *Proceedings of the IEEE/CVF conference on computer vision and pattern recognition* (pp. 11177–11185).

Mo, K., Zhu, S., Chang, A. X., Yi, L., Tripathi, S., Guibas, L. J., et al. (2019). Partnet: A large-scale benchmark for fine-grained and hierarchical part-level 3d object understanding. In *Proceedings of the IEEE/CVF conference on computer vision and pattern recognition* (pp. 909–918).

Noroozi, M., & Favaro, P. (2016). Unsupervised learning of visual representations by solving jigsaw puzzles. In *European conference on computer vision* (pp. 69–84). Springer.

Oord, A. v. d., Li, Y., & Vinyals, O. (2018). Representation learning with contrastive predictive coding. arXiv preprint arXiv:1807.03748.

Pang, Y., Wang, W., Tay, F. E., Liu, W., Tian, Y., & Yuan, L. (2022). Masked autoencoders for point cloud self-supervised learning. arXiv preprint arXiv:2203.06604.

Pathak, D., Krähenbühl, P., Donahue, J., Darrell, T., & Efros, A. A. (2016). Context encoders: Feature learning by inpainting. In *Computer vision and pattern recognition*.

Poursaeed, O., Jiang, T., Qiao, H., Xu, N., & Kim, V. G. (2020). Self-supervised learning of point clouds via orientation estimation. In *2020 international conference on 3D vision (3DV)* (pp. 1018–1028). IEEE.

Qi, C. R., Su, H., Mo, K., & Guibas, L. J. (2017). Pointnet: Deep learning on point sets for 3d classification and segmentation. In *Proceedings of the IEEE conference on computer vision and pattern recognition* (pp. 652–660).

Qi, C. R., Yi, L., Su, H., & Guibas, L. J. (2017). Pointnet++: Deep hierarchical feature learning on point sets in a metric space. *Advances in Neural Information Processing Systems, 30*.

Romera-Paredes, B., & Torr, P. (2015). An embarrassingly simple approach to zero-shot learning. In *International conference on machine learning* (pp. 2152–2161). PMLR.

Russakovsky, O., Deng, J., Su, H., Krause, J., Satheesh, S., Ma, S., et al. (2015). Imagenet large scale visual recognition challenge. *International Journal of Computer Vision, 115*, 211–252.

Sanghi, A. (2020). Info3d: Representation learning on 3d objects using mutual information maximization and contrastive learning. In *European conference on computer vision* (pp. 626–642). Springer.

Sariyildiz, M. B., Kalantidis, Y., Alahari, K., & Larlus, D. (2022). Improving the generalization of supervised models. arXiv preprint arXiv:2206.15369.

Sarmad, M., Lee, H. J., & Kim, Y. M. (2019). Rl-gan-net: A reinforcement learning agent controlled gan network for real-time point cloud shape completion. In *Proceedings of the IEEE/CVF conference on computer vision and pattern recognition* (pp. 5898–5907).

Sauder, J., & Sievers, B. (2019a). Context prediction for unsupervised deep learning on point clouds. arXiv preprint arXiv:1901.08396, 2, 5.

Sauder, J., & Sievers, B. (2019b). Self-supervised deep learning on point clouds by reconstructing space. *Advances in Neural Information Processing Systems, 32*.

Sayed, N., Brattoli, B., & Ommer, B. (2018). Cross and learn: Cross-modal self-supervision. In *German conference on pattern recognition* (pp. 228–243). Springer.

Shao, Z., Zhao, R., Yuan, S., Ding, M., & Wang, Y. (2022). Tracing the evolution of AI in the past decade and forecasting the emerging trends. *Expert Systems with Applications*, Article 118221.

Shi, Y., Cao, X., & Zhou, B. (2021). Self-supervised learning of part mobility from point cloud sequence. In *Computer graphics forum* (pp. 104–116). Wiley Online Library.

Shu, D. W., Park, S. W., & Kwon, J. (2019). 3D point cloud generative adversarial network based on tree structured graph convolutions. In *Proceedings of the IEEE/CVF international conference on computer vision* (pp. 3859–3868).

Song, S., Lichtenberg, S. P., & Xiao, J. (2015). Sun rgb-d: A rgb-d scene understanding benchmark suite. In *Proceedings of the IEEE conference on computer vision and pattern recognition* (pp. 567–576).

Stretcu, O., & Leordeanu, M. (2015). Multiple frames matching for object discovery in video. In *BMVC* (p. 3).

Sun, P., Kretzschmar, H., Dotiwalla, X., Chouard, A., Patnaik, V., Tsui, P., et al. (2020). Scalability in perception for autonomous driving: Waymo open dataset. In *Proceedings of the IEEE/CVF conference on computer vision and pattern recognition* (pp. 2446–2454).

Sun, X., Wu, J., Zhang, X., Zhang, Z., Zhang, C., Xue, T., et al. (2018). Pix3d: Dataset and methods for single-image 3d shape modeling. In *Proceedings of the IEEE conference on computer vision and pattern recognition* (pp. 2974–2983).

Sun, C., Zheng, Z., Wang, X., Xu, M., & Yang, Y. (2022). Self-supervised point cloud representation learning via separating mixed shapes. *IEEE Transactions on Multimedia*.

Taghanaki, S. A., Luo, J., Zhang, R., Wang, Y., Jayaraman, P. K., & Jatavallabhula, K. M. (2020). Robustpointset: A dataset for benchmarking robustness of point cloud classifiers. arXiv preprint arXiv:2011.11572.

Tian, H., Song, K., Li, S., Ma, S., Xu, J., & Yan, Y. (2022). Data-driven robotic visual grasping detection for unknown objects: A problem-oriented review. *Expert Systems with Applications*, Article 118624.

Tran, B., Hua, B.-S., Tran, A. T., & Hoai, M. (2022). Self-supervised learning with multi-view rendering for 3D point cloud analysis. In *Proceedings of the Asian conference on computer vision* (pp. 3086–3103).

Tsai, M.-S., Chiang, P.-Z., Tsai, Y.-H., & Chiu, W.-C. (2022). Self-supervised feature learning from partial point clouds via pose disentanglement. In *2022 IEEE/RSJ international conference on intelligent robots and systems (IROS)* (pp. 1031–1038). IEEE.

Uy, M. A., Pham, Q.-H., Hua, B.-S., Nguyen, T., & Yeung, S.-K. (2019). Revisiting point cloud classification: A new benchmark dataset and classification model on real-world data. In *Proceedings of the IEEE/CVF international conference on computer vision* (pp. 1588–1597).

Vaswani, A., Shazeer, N., Parmar, N., Uszkoreit, J., Jones, L., Gomez, A. N., et al. (2017). Attention is all you need. *Advances in Neural Information Processing Systems, 30*.

Velickovic, P., Fedus, W., Hamilton, W. L., Liò, P., Bengio, Y., & Hjelm, R. D. (2019). Deep graph infomax. *ICLR (Poster), 2*(3), 4.

Vora, S., Lang, A. H., Helou, B., & Beijbom, O. (2020). Pointpainting: Sequential fusion for 3d object detection. In *Proceedings of the IEEE/CVF conference on computer vision and pattern recognition* (pp. 4604–4612).

Wang, W., Lin, X., Feng, F., He, X., Lin, M., & Chua, T.-S. (2022). Causal representation learning for out-of-distribution recommendation. In *Proceedings of the ACM web conference 2022* (pp. 3562–3571).

Wang, H., Liu, Q., Yue, X., Lasenby, J., & Kusner, M. J. (2021). Unsupervised point cloud pre-training via occlusion completion. In *Proceedings of the IEEE/CVF international conference on computer vision* (pp. 9782–9792).

Wang, C., Ma, C., Zhu, M., & Yang, X. (2021). Pointaugmenting: Cross-modal augmentation for 3d object detection. In *Proceedings of the IEEE/CVF conference on computer vision and pattern recognition* (pp. 11794–11803).

Wang, Y., & Solomon, J. M. (2019). Prnet: Self-supervised learning for partial-to-partial registration. *Advances in Neural Information Processing Systems, 32*.

Wang, Y., Sun, Y., Liu, Z., Sarma, S. E., Bronstein, M. M., & Solomon, J. M. (2019). Dynamic graph cnn for learning on point clouds. *ACM Transactions on Graphics (tog), 38*(5), 1–12.

Wang, H., Yang, L., Rong, X., Feng, J., & Tian, Y. (2021). Self-supervised 4d spatio-temporal feature learning via order prediction of sequential point cloud clips. In *Proceedings of the IEEE/CVF winter conference on applications of computer vision* (pp. 3762–3771).

Wei, C., Liang, J., Liu, D., & Wang, F. (2022). Contrastive graph structure learning via information bottleneck for recommendation. *Advances in Neural Information Processing Systems, 35*, 20407–20420.

Wu, Z., Song, S., Khosla, A., Yu, F., Zhang, L., Tang, X., et al. (2015). 3D shapenets: A deep representation for volumetric shapes. In *Proceedings of the IEEE conference on computer vision and pattern recognition* (pp. 1912–1920).

Wu, W., Wang, Z. Y., Li, Z., Liu, W., & Fuxin, L. (2020). Pointpwc-net: Cost volume on point clouds for (self-) supervised scene flow estimation. In *European conference on computer vision* (pp. 88–107). Springer.

Wu, Z., Xiong, Y., Yu, S. X., & Lin, D. (2018). Unsupervised feature learning via non-parametric instance discrimination. In *Proceedings of the IEEE conference on computer vision and pattern recognition* (pp. 3733–3742).

Wu, B., Zhou, X., Zhao, S., Yue, X., & Keutzer, K. (2019). Squeezesegv2: Improved model structure and unsupervised domain adaptation for road-object segmentation from a lidar point cloud. In *2019 international conference on robotics and automation (ICRA)* (pp. 4376–4382). IEEE.

Xiang, Y., Kim, W., Chen, W., Ji, J., Choy, C., Su, H., et al. (2016). Objectnet3d: A large scale database for 3d object recognition. In *European conference on computer vision* (pp. 160–176). Springer.

Xiao, A., Huang, J., Guan, D., & Lu, S. (2022). Unsupervised representation learning for point clouds: A survey. arXiv preprint arXiv:2202.13589.

Xie, S., Gu, J., Guo, D., Qi, C. R., Guibas, L., & Litany, O. (2020). Pointcontrast: Unsupervised pre-training for 3d point cloud understanding. In *European conference on computer vision* (pp. 574–591). Springer.

Xie, S., Liu, S., Chen, Z., & Tu, Z. (2018). Attentional shapecontextnet for point cloud recognition. In *Proceedings of the IEEE conference on computer vision and pattern recognition* (pp. 4606–4615).

Xu, D., Xiao, J., Zhao, Z., Shao, J., Xie, D., & Zhuang, Y. (2019). Self-supervised spatiotemporal learning via video clip order prediction. In *Proceedings of the IEEE/CVF conference on computer vision and pattern recognition* (pp. 10334–10343).

Xu, M., Zhou, Z., Xu, H., Wang, Y., & Qiao, Y. (2022). Cp-net: Contour-perturbed reconstruction network for self-supervised point cloud learning. arXiv preprint arXiv:2201.08215.

Xue, L., Gao, M., Xing, C., Martín-Martín, R., Wu, J., Xiong, C., et al. (2023). ULIP: Learning a unified representation of language, images, and point clouds for 3D understanding. In *Proceedings of the IEEE/CVF conference on computer vision and pattern recognition* (pp. 1179–1189).

Yang, J., Alvarez, J. M., & Liu, M. (2021). Self-supervised learning of depth inference for multi-view stereo. In *Proceedings of the IEEE/CVF conference on computer vision and pattern recognition* (pp. 7526–7534).

Yang, Y., Feng, C., Shen, Y., & Tian, D. (2018). Foldingnet: Point cloud auto-encoder via deep grid deformation. In *Proceedings of the IEEE conference on computer vision and pattern recognition* (pp. 206–215).

Yu, X., Tang, L., Rao, Y., Huang, T., Zhou, J., & Lu, J. (2021). Point-BERT: Pre-training 3D point cloud transformers with masked point modeling. arXiv preprint arXiv:2111.14819.

Yuan, X., Shi, J., & Gu, L. (2021). A review of deep learning methods for semantic segmentation of remote sensing imagery. *Expert Systems with Applications, 169,* Article 114417.

Zamir, A. R., Sax, A., Shen, W., Guibas, L. J., Malik, J., & Savarese, S. (2018). Taskonomy: Disentangling task transfer learning. In *Proceedings of the IEEE conference on computer vision and pattern recognition* (pp. 3712–3722).

Zeng, Y., Jiang, C., Mao, J., Han, J., Ye, C., Huang, Q., et al. (2023). CLIP2: Contrastive language-image-point pretraining from real-world point cloud data. In *Proceedings of the IEEE/CVF conference on computer vision and pattern recognition* (pp. 15244–15253).

Zhang, Z., Girdhar, R., Joulin, A., & Misra, I. (2021). Self-supervised pretraining of 3d features on any point-cloud. In *Proceedings of the IEEE/CVF international conference on computer vision* (pp. 10252–10263).

Zhang, Y., Lin, J., He, C., Chen, Y., Jia, K., & Zhang, L. (2022). Masked surfel prediction for self-supervised point cloud learning. arXiv preprint arXiv:2207.03111.

Zhang, Y., Lin, J., Li, R., Jia, K., & Zhang, L. (2022). Point-DAE: Denoising autoencoders for self-supervised point cloud learning. arXiv preprint arXiv:2211.06841.

Zhang, C., Shi, J., Deng, X., & Wu, Z. (2022). Upsampling autoencoder for self-supervised point cloud learning. arXiv preprint arXiv:2203.10768.

Zhang, L., & Zhu, Z. (2019). Unsupervised feature learning for point cloud understanding by contrasting and clustering using graph convolutional neural networks. In *2019 international conference on 3D vision (3DV)* (pp. 395–404). IEEE.

Zhao, Y., Hui, L., & Xie, J. (2021). Sspu-net: Self-supervised point cloud upsampling via differentiable rendering. In *Proceedings of the 29th ACM international conference on multimedia* (pp. 2214–2223).

Zhao, W., Liu, X., Zhong, Z., Jiang, J., Gao, W., Li, G., et al. (2022). Self-supervised arbitrary-scale point clouds upsampling via implicit neural representation. In *Proceedings of the IEEE/CVF conference on computer vision and pattern recognition* (pp. 1999–2007).

Zhao, X., Yang, S., Huang, T., Chen, J., Ma, T., Li, M., et al. (2022). SuperLine3D: Self-supervised line segmentation and description for LiDAR point cloud. In *Computer vision–ECCV 2022: 17th European conference, Tel Aviv, Israel, October 23–27, 2022, Proceedings, Part IX* (pp. 263–279). Springer.

Zhou, Y., & Tuzel, O. (2018). VoxelNet: End-to-end learning for point cloud based 3D object detection. In *Computer vision and pattern recognition*.